Aus der Universität-Augenklinik Tübingen

Department für Augenheilkunde

A study to test whether intrinsically photosensitive ganglion cells (ipRGCs) activity contribute to the response to chromatic pattern ERGs

Inaugural - Dissertation

zur Erlangung des Doktorgrades der Medizin

der Medizinischen Fakultät

der Eberhard Karls Universität zu Tübingen

Vorgelegt von:

Mohammad Aloudat

aus Daraa in Syrien

2022

Dekan: Prof. Dr. Bernd Pichler

Berichterstatter: Privatdozentin Dr. A. Kurtenbach

Berichterstatter: Professorin Dr. M. Deleidi, MD, Ph.D.

Tag der Disputation: 14.08.2023

Table of Contents

Abbreviations

ipRGCs Intrinsically photosensitive ganglion cells

PERG Pattern electroretinography

OCT Optical coherence tomography

ILM Inner limiting membrane

NFL Nerve fibre layer

GCL Ganglion cell layer

IPL Inner plexiform layer

INL Inner nuclear layer

OPL Outer plexiform layer

ONL Outer nuclear layer

ELM External limiting membrane

IS / OS Inner segment / outer segment layer

RPE Retinal pigment epithelium

HC Horizontal cell

AC Amacrine cell

BC Bipolar cell

GABA Gamma-Aminobutyric acid

SC Superior colliculus

LGN Lateral geniculate nucleus

SCN Suprachiasmatic nuclei

OPN Olivary pretectal nucleus

PLR Pupillary light reflex

PIPR Post-illumination pupil response

POAG Primary open-angle glaucoma

CDR Cup-to-disc ratio

IOP Intraocular pressure

VF Visual field

C/D ratio Cup-to-disc ratio

LED Light-emitting diode

LCD Liquid Crystal Display

DTL Dawson, Trick, and Litzkow

ISCEV International Society for Clinical Electrophysiology of Vision

EEG Electroencephalography

SAS Statistical analysis system

Amp Amplitude

Imp Implicit time

CC Correlation Coefficient

1. Introduction

1.1 The visual system

1.1.1 Neurons

Neurons play a major role in the functioning of the nervous system. They generate and transmit neurological signals and transport them further to other cells. Based on their function, we can generally classify neurons into three groups:

1 Motor neurons that play the main role in the functioning of the musculoskeletal system, as they can stimulate all forms of muscle cells.

2 Sensory neurons that are sensitive to sensory stimulation. Via the nerves, these neurons transmit information from the receptors in the sensory or other organs to the brain and spinal cord.

3 Interneurons (intermediate neurons). These neurons can provide communication between two or more nerve cells, including motor neurons and sensory neurons (Nicholls et al., 1992).

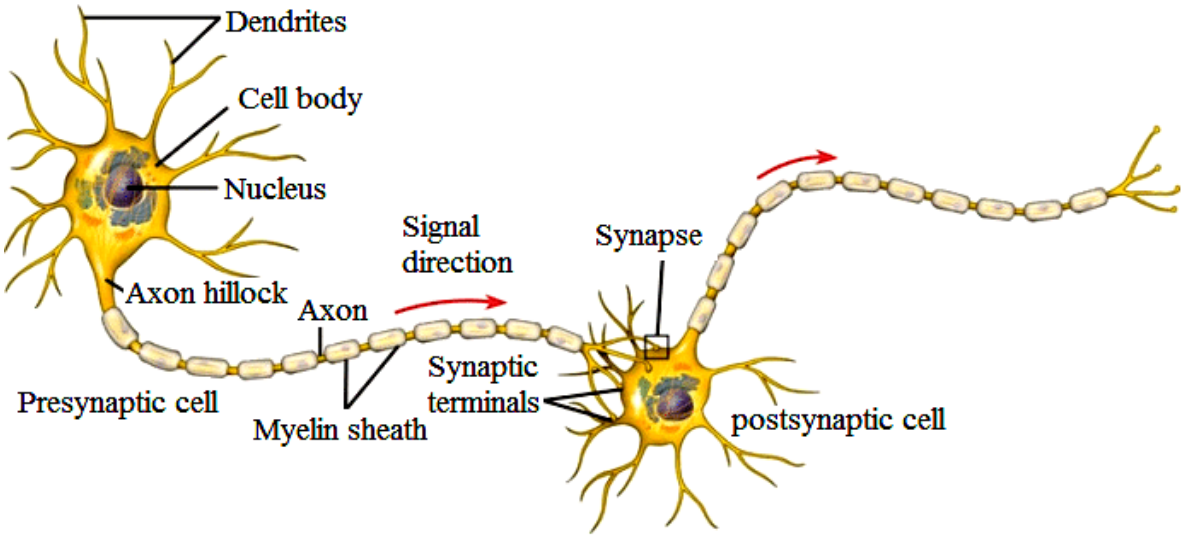

Figure 1. Structure of the typical neuron (Torse, Maggavi, & Pujari, 2012). Left is the cell body with its nucleus and dendrites. Its axon transports the signal via synapses to a postsynaptic cell (right) which transport the signal

The neuron is the main structure of the nervous system and consists of 3 important sub-parts, a cell body, an axon and dendrites. This is depicted in Fig. 1. All neurons have a cell body which contains the cell nucleus. All proteins and other important substances that are necessary for the functioning of the nerve cell are formed in the cell body. In addition, the cell body also has various organelles such as mitochondria, the Golgi apparatus etc. The dendrites are plasmatic processes that grow outward from the cell body and form contact points for other cells. That is why the dendrites play an important role as chemical and electrical signal receivers, which can receive and transmit many messages and excitations from other neurons through the synapse. The function of the axon ensures the transport of signals from cell body to cell body. Long axons have increased transmission speeds because they are usually covered with a myelin sheath.

1.1.2 The retina

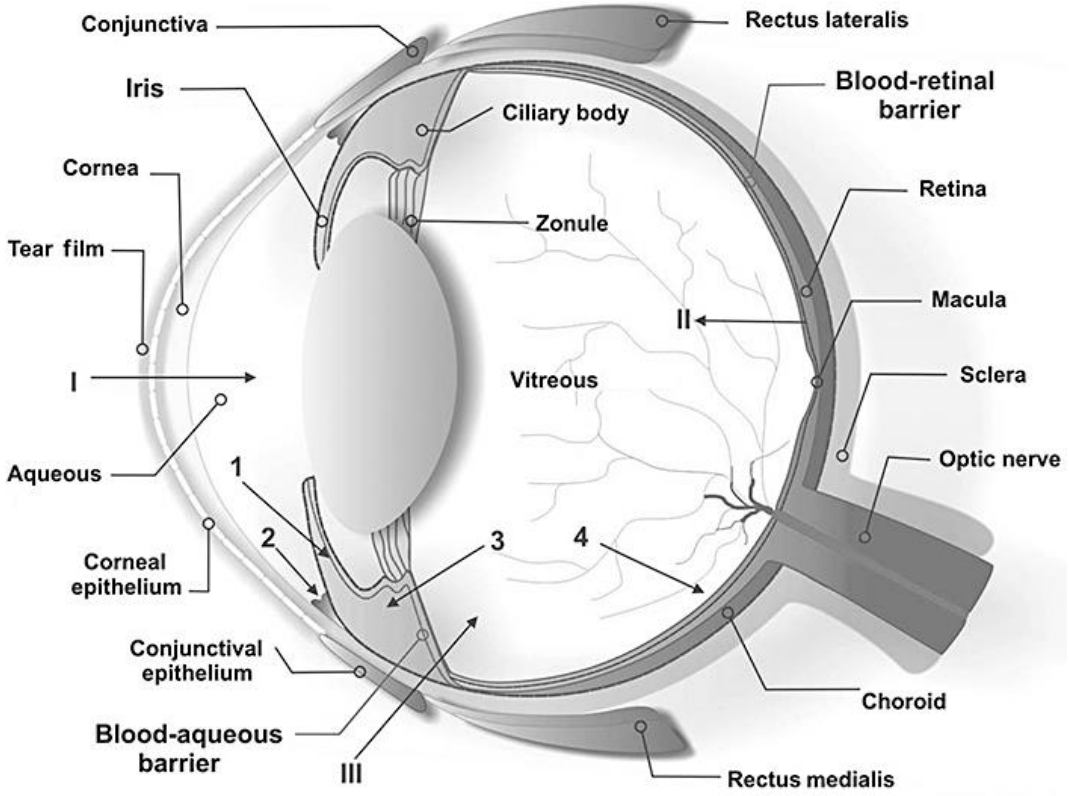

Figure 2. Anatomy of the Eye (Willoughby et al., 2010). The two halves of the eye can be seen. The anterior focusses the incoming light onto the posterior of the eye, where the retina is situated.

Vision is one of our most importance senses. It supplies the individual with accurate information about the environment and thereby allows us to interact with our surroundings and to navigate. As well as these image forming functions, there are more subtle functions of vision, such as the adaptation of the individual to diurnal rhythms and the overall brightness of the environment. All of these functions, image forming and non-image forming, are processed in different visual areas of the brain. The first steps of this processing occurs already in the eye. The eye can be functionally split into two halves (see Fig. 2). The anterior half includes the cornea, iris, lens and ciliary body which together focus light onto the posterior half of the eye. The wall of the eyeball contains three main layers: an outer fibrous layer (the sclera), a middle vascular layer (the choroid) and an inner nervous tissue layer (the retina). Bruch's membrane separates the retina from the outer choroidal capillary network.

The human retina has a laminar structure with a thickness of 200 – 300 µm, which, apart from neurons, consists of three dominant types of glial cells: Müller cells, astrocytes and microglia that provide support and protection (Dowling & Boycott, 1966).

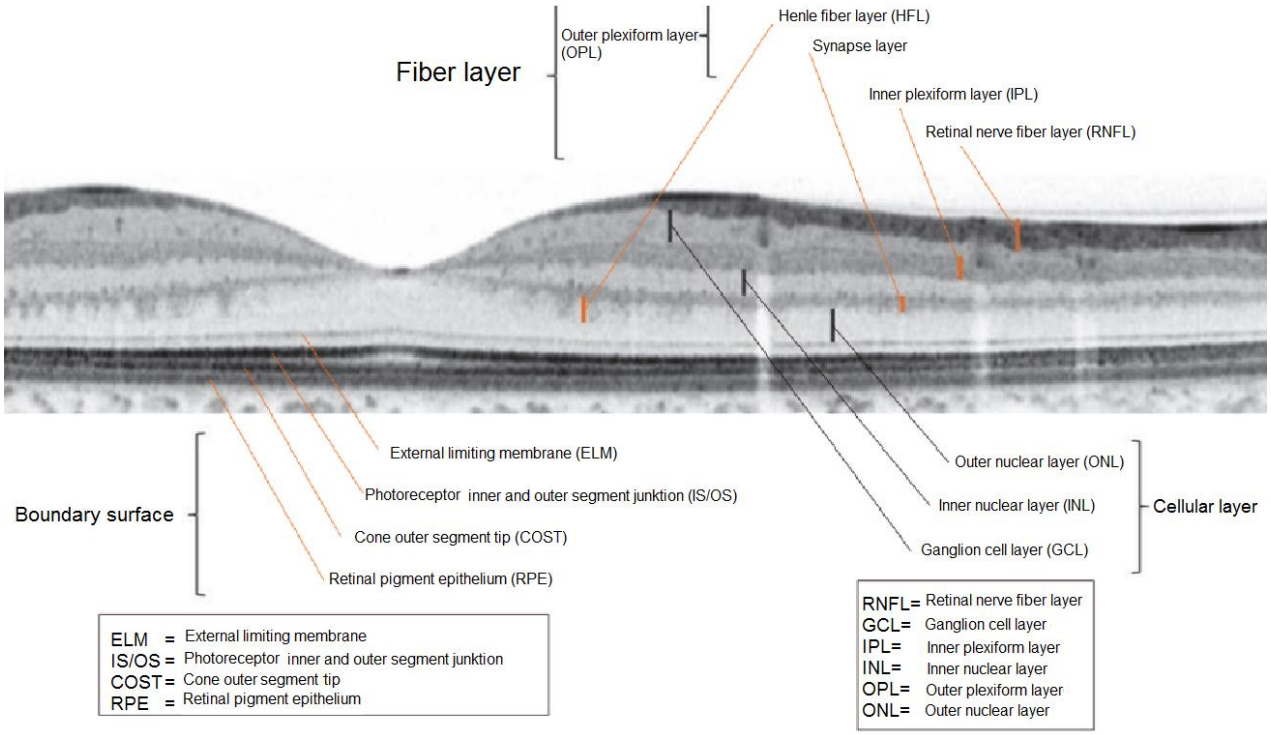

Figure 3. Retinal layers in an OCT image (from OCT Atlas by Nagahisa & Hangai, 2012). There are 10 layers stretching from the RPE (lower dark layer) to the outer limiting membrane. The fovea is marked by the small depression.

The neurosensory retina is a thin translucent tissue that varies in thickness from 0.5 mm at the disc to 0.1 mm at the ora serrata. It is firmly joined to the RPE at the ora serrata and the optic nerve head and is held in place in the intermediate regions of the eye by intraocular pressure. The retina can be differentiated into ten different layers, which are depicted in the OCT image in Fig. 3. The outer nuclear layer (ONL) mainly contains the cell bodies of photoreceptors. The inner and outer segments (IS, OS) of the photoreceptors lie in the photoreceptor layer (PR) between the ONL and the retinal pigment epithelium (RP). The outer limiting membrane (OLM) is located between the plasma membranes of the inner segments and the apical processes of Müller glia. The OLM comprises a series of zonula adherence junctional complexes which seal off the light-sensitive photoreceptor inner and outer segments from the rest of the retina, limiting the diffusion of phototransduction cascade components (West et al., 2008). The outer plexiform layer (OPL) consists of a heavy network of synaptic contacts between photoreceptor cells and neurons of the inner nuclear layer, whereas the inner nuclear layer (INL) mainly contains the following cells: horizontal cells, bipolar cells, amacrine cells, Müller cells and glial cells. The inner plexiform layer (IPL) is a network consisting of the following components: dendrites of ganglion cells, dendrites of amacrine cells and axons of bipolar cells. At this stage, the information is preprocessed before it is transported to the brain. The ganglion cell layer (GCL) contains cell bodies of the ganglion cells and displaced amacrine cells. Ganglion cells receive signals from the bipolar cells and the amacrine cells at the border of the inner plexiform layer (IPL), and so the signals are transmitted through the axons of the ganglion cells to regions in the brain. These axons collect and then form the optic nerve fiber layer (NFL).

1.1.3 The retinal pigment epithelium and photoreceptors

The photoreceptors detect light and the pigment epithelial cells provide their metabolic support. The pigment cells contain opsins which strongly absorb light in the range 400-800nm. The pigment epithelium serves to limit the amount of light reflected or scattered within the eye. In addition, the pigment epithelium is involved in the active transport of metabolites, the provision of a blood-retinal barrier and the regeneration of photoreceptor pigments and phagocytosis. Rods are characterized by an extensive convergence of

signals onto ganglion cells. This optimizes their sensitivity, but their large receptive field sizes (areas of convergence) result in poor resolution. The photopigment rhodopsin in rods has two components; retinal, a light absorbing molecule closely related to vitamin A, attached to opsin a protein moiety that has differing forms. Light absorption breaks rhodopsin down into these two components. The transduction cascade causes a decrease in Na+ conductance in the outer segment plasma membrane. Light therefore prevents the leakage of Na and the receptor hyperpolarises. Excitation is conveyed in the retina as an initial inhibitory, graded hyperpolarisation of the receptors the inner segments transmit information to the bipolar and horizontal cells. The synaptic bodies are called rod spherules or cone pedicles.

Individual cones contain one of three visual pigments whose absorption spectra are maximal for red, green or blue of wavelengths 570nm, 535nm and 445nm respectively. Anatomically both rods and cones may be differentiated into inner and outer segments which are connected by a thin cytoplasmic bridge. Light sensitive pigments are located in the outer segments in an elaborate system of stacked membraneous discs that interdigitate with the pigment epithelium. These numerous membraneous invaginations increase the effective surface area of photopigment molecules and facilitates the maximum interaction with light. Cone discs remain connected with the surface membrane. Rod discs separate from the outer membrane and undergo constant renewal. They disintegrate at their apical surface and are phagocytosed by the pigment epithelium. New discs migrate from the basal pole to replace those lost.

The synaptic layer is termed the outer plexiform layer. Cones send out processes that end on nearby cone pedicles and rod spherules. These inter-terminal receptor contacts resemble gap junctions and allow an electrotonic spread of current between adjacent cells. There is also evidence in the macula region that other connections occur across receptor inner segments, but the nature of the contact has not been defined. In the cat retina transmitter release is mediated at the cone axon terminal. The source of the input is not important, thus, under photopic conditions the cone outer segment transduces light. At low luminances the transduction occurs in the rod outer segment and is conveyed to the cone terminal via gap junctions. Initially therefore there is not much change in the ganglion cell receptive field. However, with dark adaptation the surround antagonism

weakens and the ganglion cell receptive field centre becomes very sensitive. The ganglion cell may then linearly spatially summate quantal events that arise in individual rods. This suggests that the rod cone gap junctions close after prolonged dark adaptation and that the rod to rod bipolar synapse conducts the information.

The human fovea morphologically matures to form the foveal depression via the peripheral migration of displacement of the inner retinal layers. The full extent of the depression in humans is 5° arc or 1.5mm on the retina. The central rod free zone decreases to less than 0.4 mm2 (54' arc extent) in adult retinae following a central 'migration of displacement' of cones. A concomitant elongation and thinning of the foveal cones also serves to increase cone packing. The photoreceptor axons, the Henle fibres, are swept horizontally as they leave the foveal area. The horizontal and bipolar cells with which they interact and the amacrine and ganglion cells that receive information from the foveal cones are also centrifugally and laterally displaced. There is considerable evidence to suggest that the packing density of adult primate foveal photoreceptors sets the limit for the transmission of spatial frequency by the retina.

1.1.4 Inner nuclear layer

The inner nuclear layer contains the cell bodies of the horizontal, bipolar and amacrine cells.

1.1.4.1 Horizontal cells

The axons and dendrites of the horizontal cells lie in the inner part of the outer plexiform layer, while the bodies of the cells lie in the outer part of the inner nuclear layer. The cells have shorter dendrites in the centre where they are more densely packed (Duke-Elder & Wybar, 1961). Morphologically we can distinguish three different forms of horizontal cells:

1. The external horizontal cells (HCs) which are closest to the photoreceptors and receive an exclusive input from cones. They may be subdivided into distal luminosity L-type cells that hyperpolarize to all wavelengths, and more proximal chromaticity C-type horizontal cells which depolarize to some colours and hyperpolarize to others (MacNichol & Svaetichin 1958).

2. The intermediate horizontal cells that receive an exclusive rod input and modify transmission from rod bipolars.
3. The internal horizontal cells which are now considered the processes of the external horizontal cells.

As a generalization of the mammalian retina, the axon terminals of HCs end exclusively in the rod terminal, where a single bipolar cell process is flanked by two lateral HC processes within the rod spherule. Conversely, the dendritic terminals of HCs connect exclusively to cone pedicles, thus forming a unidirectional signal transduction pathway. The main function of horizontal cells is the formation of the circuits between the bipolar cells and photoreceptors, and here the signals are possibly inhibited by the lateral inhibitory pathways. The horizontal cells can change the light adaptation of the eye so that the image contrast is improved.

1.1.4.2 Bipolar cells

The cell bodies of the bipolar cells are located in the inner nuclear layer and make up the highest number of neurons in this layer. Bipolar cells have many synaptic connections with photoreceptors. With the help of these synapses, the bipolar cells take information from photoreceptors and pass this information on to ganglion cells. There are at least ten subtypes of bipolar cells, one of which synapses exclusively with rod photoreceptors, whereas the others are cone-related (Kolb et al., 1981). The synapses can be one of three basic forms:

1. Ribbon synapses: These synapses have an electron dense bar called the pre-synaptic ribbon which is perpendicularly oriented to the pre-synaptic membrane. This ribbon is intimately associated with synaptic vesicles. The bipolar making this synaptic connection deeply invaginates the pedicle or spherule and is consequently named the invaginating bipolar cell. Typically ribbon synapses involve three post synaptic elements. The triad is formed by two horizontal cells laterally and an invaginating bipolar cell centrally (Dowling & Boycott, 1966).

2. Superficial or flat synapses: Flat synapses only involve one non-invaginating post synaptic element.

3. Conventional or electrical synapses: These are gap junctions which can occur between receptors and at their terminals.

Bipolar cells are functionally divided in OFF- and ON-bipolar cells. OFF-bipolar cells express ionotropic glutamate receptors on their dendritic tips, which are located on the base of the cone pedicles. They respond to the offset of light following an increase of glutamate released by photoreceptors and are hence sign-conserving. ON-bipolar cells, in contrast, express metabotropic glutamate receptors on their dendritic tips and are depolarized at the onset of light, caused by a reduction of the glutamate release from the photoreceptors in response to light. ON-bipolar cells make invaginating contacts beneath the synaptic ribbons of the photoreceptor terminals (cone pedicles and rod spherules) with their dendrite. It was also demonstrated that some ON-bipolar cells make additional basal contacts to the cone pedicle, but the majority of their contacts are invaginating (Hopkins & Boycott, 1997).

1.1.4.3 Amacrine cells

Amacrines act as intermediaries between bipolar and ganglion cells. They are inhibitory interneurons of the inner retina, which receive glutamatergic synaptic input from bipolar cells and inhibitory inputs from other amacrine cells within the IPL. They may synapse individually with each cell type or contact both simultaneously in a dyad. Amacrine cells provide synaptic output to ganglion cells, bipolar cells as well as other amacrine cells and thereby control the output from bipolar cells onto ganglion cells or directly modulate ganglion cell responses. Most amacrine cells use glycine or GABA as their neurotransmitter and are thought to modulate the responses of target cells via inhibitory synaptic input. A plethora of different amacrine cell types has been described morphologically and functionally in various species (see Masland, 2001).

Amacrine cells are usually classified according to their dendritic field size and stratification. However, they can be coarsely sub-divided into wide-field amacrine and small-field amacrine cells. Wide-field amacrine cells are characterised by large monostratifed dendritic arbors, which are restricted to narrow sublaminae of the IPL. As their primary neurotransmitter, wide-feld amacrine cells use GABA and can be immunohistochemically labelled using antibodies against GABA or its synthesising enzyme glutamic acid decarboxylase.Small-feld amacrine cells, in contrast, use glycine as their neurotransmitter and their dendritic trees occupy only small lateral areas (10 - 100 µm in diameter) within the IPL.There is also a sustained or true amacrine that lacks

an axon and produces slow sustained potentials without spike activity. There are also transient amacrine cells that are bistratified and act as frequency doublers giving non-linear responses. The transient amacrines have been described as intraretinal ganglion cells (Chan & Naka 1976).

It is probable that the nature of the amacrine cell response depends on the inner plexiform layer sublamina in which it receives its functional input i.e. on the centre sign of the bipolar or ganglion cell (Zrenner et al., 1983). Wide field amacrines seem to interact in a lateral network within a single sublamina synapsing with ganglion cell dendrites in that stratum. Bistratified amacrines have a distinct neurocircuitry for each of the two sublamina in which they ramify, but appear to be involved in information flow in a vertical rather than lateral direction (Kolb et al., 1981). Other amacrines make reciprocal synapses with neighbouring bipolar cells and probably participate in feedback circuits (Nakatsuka & Hamasaki, 1985).

1.1.5 Ganglion cell layer

1.1.5.1 Retinal Ganglion Cells

Hartline was awarded the Nobel Prize in 1967 for his investigation of ganglion cell receptive fields. The receptive field defines the spatial characteristic of a ganglion cell. Examining the mammalian eye, Kuffler (1953) described symmetrically concentric centre-surround cat ganglion cell receptive fields. The ganglion cells responded to a light spot with either an excitatory ON-centre or an inhibitory OFF-centre, whilst the surround of the receptive field gave an antagonistic or opposite response. In the simplest receptive field model, the signals from the centre surround mechanisms are summed, with Gaussian weighting functions, to provide the output of the ganglion cells. A delay in the surround signal relative to the centre signal is necessarily introduced in such models to explain the spatio-temporal interactions of a cell, although the general form of its temporal frequency response characteristic is probably provided by the characteristics of elements common to both centre and surround.

Ganglion cells represent the output of information from the retina. They receive glutamatergic synaptic input from bipolar cells and are modulated by inhibitory synaptic input from glycinergic and GABAergic amacrine cells. In turn the ganglion cells send

their signal via their axons through the optic nerve to higher brain areas, such as the LGN or the suprachiasmatic nucleus, for further processing.

Physiologically, ganglion cells form a highly diverse group. In a first categorisation, ganglion cells can be divided into ON- and OFF-ganglion cells which respond to light onset or offset only. This classification is based on the stratification depth of dendrites within the IPL. Ganglion cells associated with OFF bipolar cells collect in the OFF layer of the IPL. Ganglion cells responding to the onset of light, in contrast, branch within the ON-layer and receive input from ON-bipolar cells. Bistratifed ganglion cells with dendritic trees branching in both layers display ON/OFF responses to appropriate stimulation (see Glaser et al., 1999).

There are three different forms of ganglion cells in the retina: midget (P cells), parasol cells (M cells) and bistratified cells (K cells). The midget cells have small cell bodies with a tiny dendrite tree and make up about 80% of the total ganglion cells in the retina. Parasol cells have a larger cell body with a larger dendrite tree and these cells make up about 10% of the total ganglion cells in the retina. Bistratified cells have a much larger dendrite tree compared to other cells. Axons of midget cells and parasol cells project to the lateral geniculate nucleus (LGN). Functionally there is also a big difference between parasol cells and midget cells: Parasol cells have large receptive fields and are responsible for differentiating between lightness and darkness, while midget cells have small receptive fields and are responsible for differentiating the red / green contrast (Watanabe & Rodieck, 1989).

1.1.5.2 The discovery of a non-visual photopigment (melanopsin)

In 1991 Foster and colleagues found that in a mutant strain of mice, with severe degeneration of the photoreceptor layer (*rd/rd*), circadian rhythm entrainment still occurred, indicating that some form of “light detection” was still possible.

This photoreception was shown to be dependent on melanopsin, which is expressed uniquely in intrinsic photosensitive ganglion cells, ipRGCs (Provencio et al., 2000: Hattar et al., 2002) and has been shown to be involved in the biological clock (Provencio et al., 1998). ipRGCs make up only around 1% of ganglion cells and are distributed over the entire retina. Berson et al, (2002) has described the properties of ipRGCs such as spectral tuning, kinetics and sensitivity. The ipRGCs were shown to be selectively

sensitive to short-wave light with a high sensitivity at 480 nm (blue light). They have a higher density around the macular area except for the foveola, which has almost no ipRGCs and around 95% of the cell bodies of ipRGCs lie in the GCL with the remainder in the INL (Dacey et al., 2005).

1.1.5.3 Morphological features of ipRGCs

There are at least five types of ipRGCs in humans: M1, M2, M3, M4 and M5, each with distinct properties (see Lee & Schmidt, 2018). These are depicted in Fig.4, along with their dendritic stratification. The type M1 ipRGC differ from type M2 in that their dendrites stratify in the outer sublamina (OFF sublamina) of the IPL and do not stratify in the inner sublamina (ON sublamina). In addition, M2 ipRGCs have relatively larger cell bodies and larger dendrites compared to M1 cells (Warren et al., 2003).

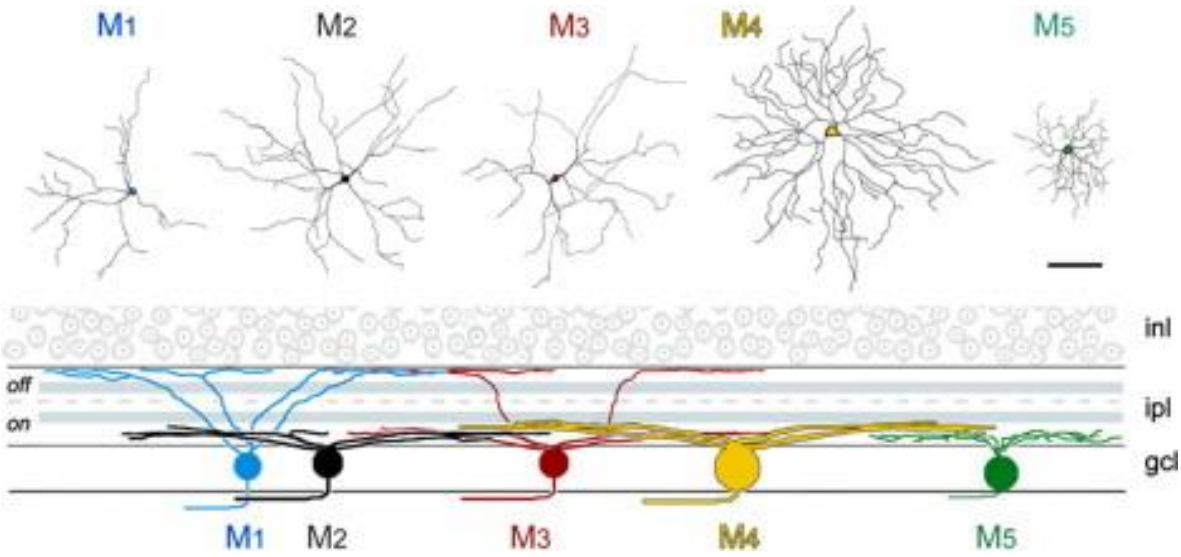

Figure 4. Morphology of ipRGCs (from Cui et al., 2015). The upper panel shows the morphology of the 5 different cell types, the lower panel shows their dendritic stratification (inl: inner nuclear laye; ipl: inner plexiform layer; gcl:ganglion cell layer). There are 2 bands of melanopsin dendrites.

The dendrites of the M3 cells are located in both sublamina of the IPL (OFF and ON). The dendrites and the cell body size are similar to that of M2 cells (Schmidt et al., 2011). Type M4 has the largest cell bodies and dendrites. Type M5 has small dendrites and both M4 and M5 types are in the ON sublamina of the IPL (Ecker et al., 2010). Types M4 and

M5 also have lower levels of melanopsin compared to other ipRGCs (Estevez et al., 2012)

1.1.5.4 Function of ipRGCs

The activity of the ipRGCs integrates with that of the other photoreceptors to provide a combined signal that transports information about luminance and light conditions. One primary role is to signal light for largely subconscious, non-image-forming visual reflexes like total light levels over long time periods (Dacey et al, 2005), although a role in form vision has recently been proposed (Allen et al. 2019). Melanopsin and rod signals have been shown to signal low light levels (Lee 2019) and opponent signals have been found between melanopsin and S-cone activity (Spitschan et al 2014, Zele 2018,).) as well as between S-cone input and M and L cones (Spitschan et al, 2014).

ipRGCs also play a major role in regulating the circadian rhythm. This fact was initially suspected because removal of the eyes in mice abolished circadian behaviour, whereas mice lacking rod and cones retained their daily rhythms (Freedman et al., 1999). The involvement of the ipRGCs axons in the retinohypothalamic tract has also been established. This tract connects the retina with the superior chiasmatic nucleus, which is known as the endogenous circadian center (Hannibal et al., 2004). A further major role of ipRGCs is to regulate pupil size through the pupillary light reflex (PLR), which is described below.

In this thesis I concentrate on the activity of this subclass of ganglion cell.

1.2 Pupillary light reflex (PLR)

ipRGCs provide information to the olivary pretectal nucleus (OPN) which forms the afferent part of the pupillary light reflex (Hattar et al., 2002). Because the PLR does not rely on the activity of the photoreceptors, blind patients with rod or cone degeneration can have intact reflexes. It has also been confirmed that the PLR is completely abolished upon ablation of ipRGCs in the retina of mice (Hatori et al., 2008). A light stimulus first leads to rapid pupil constriction up to the maximum pupil constriction, followed by

gradual pupil expansion (pupil escape) up to a firm and stable pupil constriction (Kawasaki et al., 2007).

The pupil constriction after the light stimulus has ended, the Post-Illumination Pupil Response (PIPR) is attributed to the activity of melanopsin, which has been shown to be important for the rapid phase of maximum pupil constriction and for complete pupil constriction (Gooley et al., 2001, McDougal & Gamlin, 2010).

Fig. 5 depicts the course of the PIPR response along with its metrics. The peak constriction (8 in Fig.5) and time to peak (9 in Fig.5) along with redilation time (14 in Fig.5) are the main parameters.

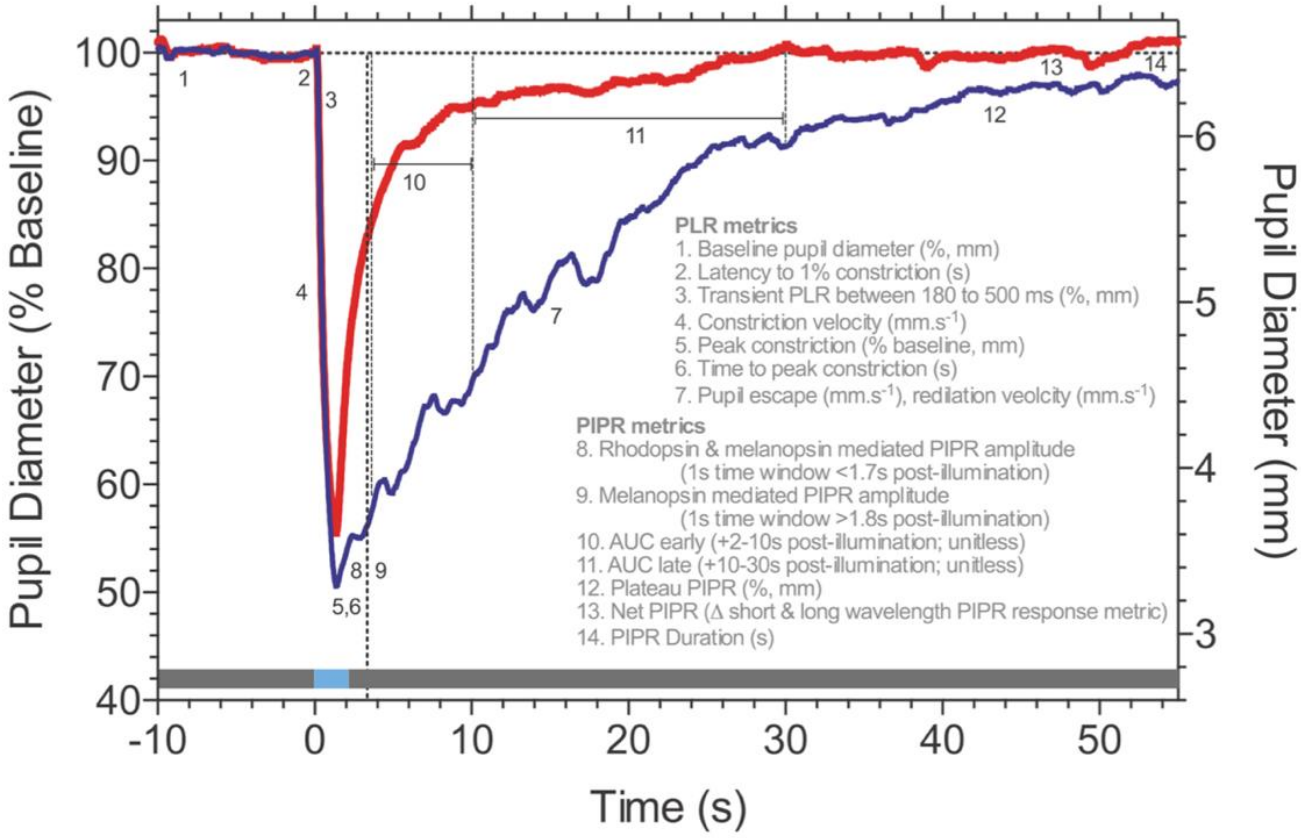

Figure 5 Parameters of the PLR and PIPR (from Kelbsch et al., 2019: Pupil diameter is plotted as a function of time. Consensual pupillary responses after 1 sec stimulation with red (red lines) or blue (blue lines) light.

The pupillary light reflex consists of rhodopsin-driven rod responses, opsin-driven cone responses and melanopsin- driven ipRGC responses (Berson et al., 2002, Hattar et al., 2003, Dacey 2005 et al., Gamlin et al., 2007). The early response (PIPR</=1.7 s) is mainly due to

melanopsin and rhodopsin with smaller amounts of cone response, whereas the later response
(PIPR</= 1.8 s) is entirely melanopsin driven (Park et al., 2011, Adhikar et al., 2015). The red stimulus under light adaptation conditions will favour cone responses, whereas a blue stimulus under dark adapted conditions will favour rod and melanopsin.

1.3 Aim of this study

The increasing role of ipRGCs in visual processing leads to the question of their possible contribution to electrophysiological recordings of retinal activity. Especially the pattern electroretinogram (PERG) elicits activity predominantly in the ganglion cells of the inner retina, but whether ipRGCs are involved in the response is not known, and is difficult to ascertain given that the spectral sensitivity of melanopsin overlaps those of both rods and S-cones. An interaction between melanopsin and S-cones has been reported (Spitschan et al., 2014). In this study, we first aimed to record the S-cone contribution to the PERG. It has been shown that a small S-cone activity can be recorded with suitable parameters; i. e. adaptation to a yellow background before recording with a (Niepel & Dodt, 1989). As the S-cone and melanopsin have similar spectral sensitivities we hypothesise that this peak also contains melanopsin activity. Secondly, we sought to correlate this S-cone activity to the activity of melanopsin recorded by the pupil response, again to coloured stimuli (Gooley et al., 2001, McDougal & Gamlin, 2010). A correlation between these measures might indicate that melanopsin pariticipates in the S-cone peak of the PERG. Additionally, blood pressure, O_2 and pulse were measured before, between and at the end of the recordings to ensure that alterations in these parameters do not influence the data.

The aim of this project, therefore, is to test whether the transient PERG to blue stimulation also invokes the activity of ipRGCs. Recordings from normal subjects as well as from patients with glaucoma, who have been shown to have dysfunctional ipRGC-mediated responses (Kankipati et al., 2011), were compared and analysed for correlations between PERG and pupillometry parameters.

2. Materials and Methods

2.1 Patients

Fifteen healthy control subjects were recruited into the study and 15 patients with glaucoma. Only one eye was included for analysis.

2.1.1. Inclusion and exclusion criteria

2.1.1.2 Inclusion criteria

Control Subjects: Corrected visual acuity ≧ 1.0, age 18 - 70 years, no suspected or confirmed eye disease (anamnesis), agreement to participate in the study, intraocular pressure > 22 mmHg or < 10 mmHg.

Patients: No suspected or confirmed eye disease, other than moderate or advanced glaucoma, age 18 - 70 years. All patients were diagnosed to have primary open-angle glaucoma (POAG) (patients with at least two of the following criteria: visual field defect not explainable by other causes, the cup-to-disc ratio (CDR) > 0.8 or an asymmetry in CDR > 0.2, intraocular pressure (IOP) > 22 mm Hg, or IOP lowering treatment) (22 eyes of 11 patients), glaucoma suspects (one of the following in at least one eye in an individual with open anterior chamber angles by gonioscopy; appearance of the optic disk or retinal nerve fiber layer that is suspicious for glaucomatous damage, a visual field suspicious for glaucomatous damage in the absence of clinical signs of other optic neuropathies or consistently elevated IOP associated with normal appearance of the optic disk and retinal nerve fiber layer and with normal visual field test results) All glaucoma patients had received pressure-lowering topical treatment in both eyes and all persons were phakic.

2.1.1.3 Exclusion criteria of control subjects and patients

Epilepsy, persons who are incapable of giving consent, minors < 18 years old, refraction spherical > ±5 diopters or cylindrical diopters > ±3, pregnancy, psychotherapeutic drugs or other medication that could influence the examinations.

The inclusion and exclusion criteria were controlled for during the initial examination (below).

2.1.2 Recruitment

Control subjects: Healthy individuals were mainly chosen from a list of those previously recruited for other studies in the Eye Hospital. They were either sent the Subject Information Form per e-mail or spoken to directly. If they were interested in participating in the study, an appointment was made.

Patients: Based on their clinical records, suitable glaucoma patients attending the University Eye Hospital were asked if they were interested in participating in the short test. If so, they were handed the Patients information form to read. After a period of 1-2 hours, in which time they could consider their decision, they were asked if they wish to participate and were either examined immediately or an appointment made. The clinical records of the glaucoma patients showed that all had glaucomatous optic discs (increased C/D ratio with localized loss or thinning of neuroretinal rim, generalized loss of disc rim, or peripapillary disc hemorrhage) and visual field (VF) defects. Glaucomatous visual field (VF) defects satisfied the following the conditions: glaucoma hemifield test results were outside normal limits at either ≥ 3 adjacent points with $p < 0.05$ or ≥ 2 adjacent points with $p < 0.02$ on a pattern deviation probability map. We considered the VF results reliable when fixation loss was < 20%, the false-positive rate was < 15%, and the false-negative rate was < 15%.

2.1.3 Sample size

The study compares parameters from 2 experimental methods and 2 groups of subjects. Assessment of an effect are based on paired correlations (Bland-Altman plots) to analyse the relation between the PERG and pupillometry parameters, using the data from one eye for statistical analysis. In this explorative study, the data from 15 subjects and 15 patients is initially sufficient to allow statistical testing.

2.1.4 Initial examination

Anamnesis included verifying the inclusion and exclusion criteria and a basic ophthalmological examination, including slit lamp examination of the anterior segment of the eye, refraction (Möller Wedel®), fundus examination (Volk 90D, non-contact

Slitlamp Lens) and intraocular pressure (Goldmann tonometer, Haag-Streit, Bern, Switzerland).

After the anamnesis, the subject, if suitable for the study was recruited ensuring that all his/her questions and queries about the study have been answered. They were then given, the Agreement of Participation form to read and sign. They were either examined immediately or returned after an appointment for the examination had been agreed upon.

2.2 Experimental procedures

2.2.1 Pattern ERG

The ISCEV (International Society for Clinical Electrophysiology of Vision) standard PERG is derived largely from the macular retinal ganglion cells. The PERG waveform in normal subjects usually consists of a small initial negative component with a peak time of approximately 35 ms (N35), followed at 45–60 ms by a much larger positive component This positive component is followed by a large negative component at 90–100 ms (N95. It has been shown that the P50 wave arises from RGC body and the N95 wave arises from RGC axon (Bach et al., 2018).

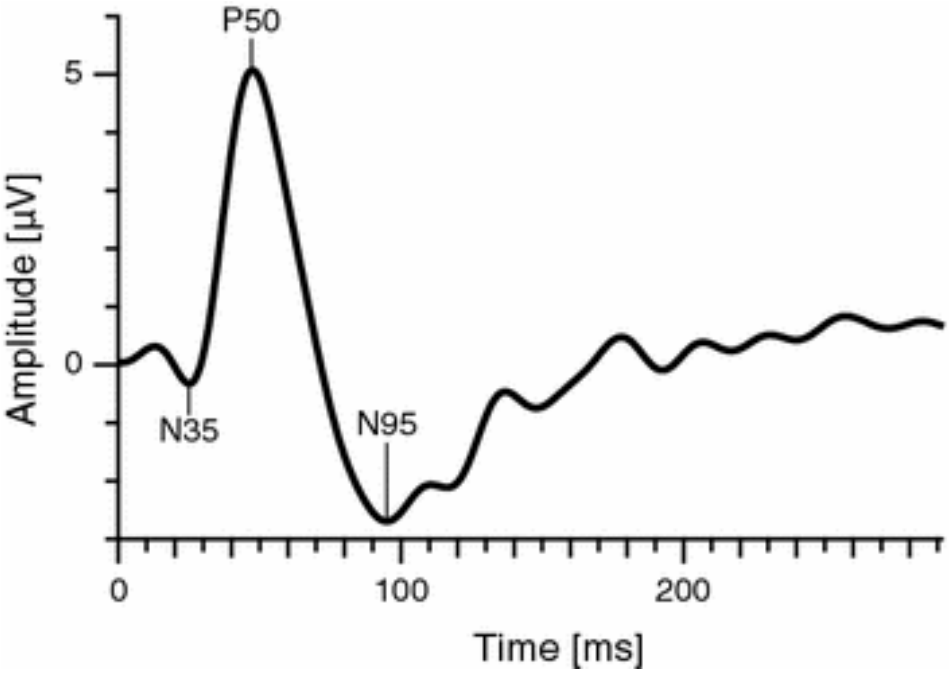

Figure 6: Schematic diagram of a standard transient PERG (Bach et al., 2013) There are 2 troughs at 35 (N35) and 95 ms (N95) and one main peak at 50 ms (P50).

The amplitudes of the standard PERG components are normally measured between peaks and troughs. The P50 amplitude is measured from the trough of N35 to the peak of P50. The N95 amplitude is measured from the peak of P50 to the trough of N95. It should be recognized that measured in this way, N95 amplitude includes the P50 amplitude and P50 that of N35. In cases where the N35 is poorly defined, the P50 amplitude is measured from the average baseline (between time zero and the onset of P50) to its peak (Bach et al., 2013).

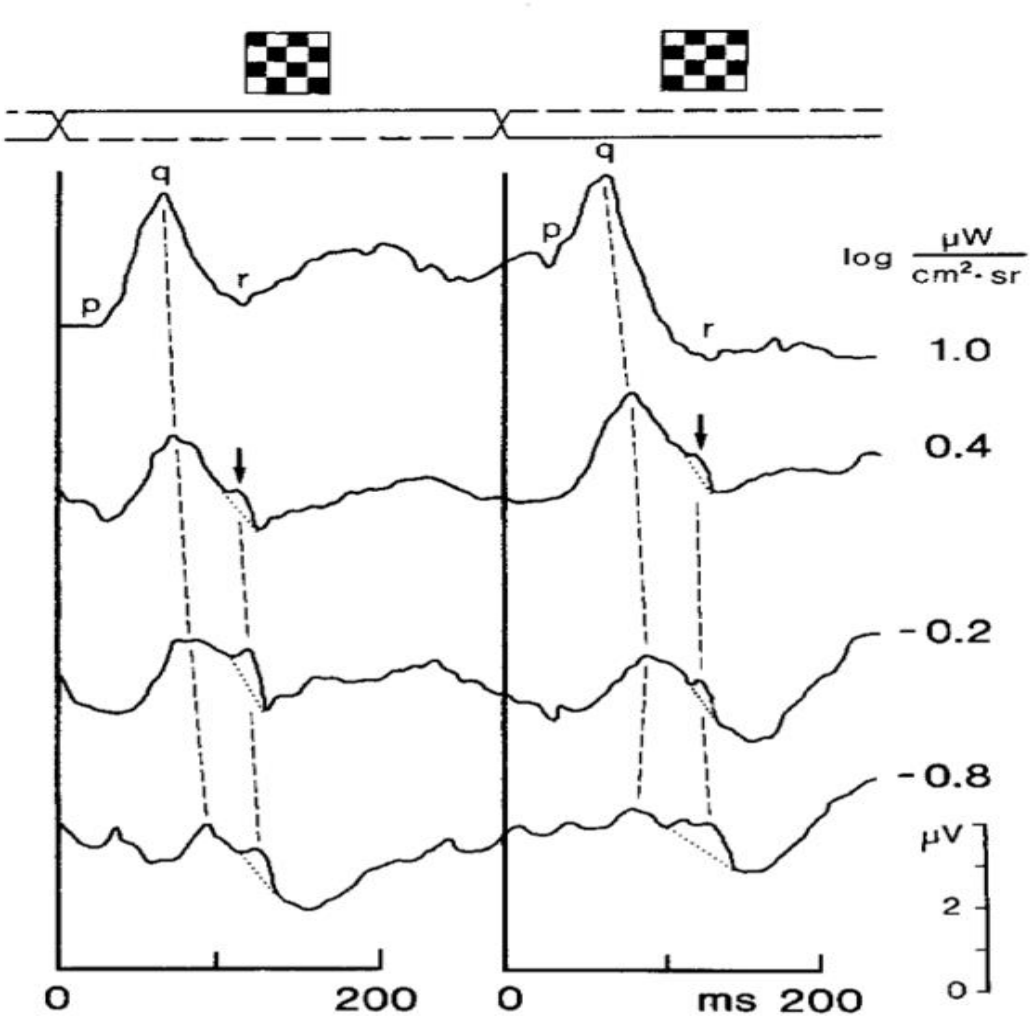

Figure 7 PERG recordings to blue-black checkerboards. The S-cone response is indicated by the arrow, p = N35, q = P50, r = N95 (Niepel & Dodt, 1989).

To obtain the S-cone peak (P), yellow light adaptation is necessary and blue-black checkerboard stimulation which delays the P50 and N95 somewhat. P is to be found on the decline after the P50 peak with an implicit time of between 90-110 ms (Niepel & Dodt,1989) as shown in Fig. 7. To measure its amplitude, we subtracted the amplitude of the P1 peak from that of the P50, meaning that the larger the difference, the smaller P1 is.

PERG are routinely recorded in the clinic in accordance with ISCEV guidelines Bach et al., 2012). To record the PERG, corneal DTL fibre electrodes (Dawson, Trick, and Litzkow electrodes) are placed along the edge of the lower lid and fixed with sticking plaster onto the skin at the right and left corners of the eye. One drop of local anaesthetic is applied beforehand (Novesine 0.5%, Omnivision: active ingredient Oxybuprocain-HCl). Additionally, one silver cup reference electrode is fixed to each temple and one to the centre of the forehead. Before attaching these electrodes, the skin is cleaned with abrasive paste to ensure low impedance. Recordings from both eyes simultaneously was performed using the Espion e² system (Diagnosys UK Ltd., Cambridge, UK). The signals were recorded on a Espion V6 by Diagnosys and stored for later analysis.

2.2.1.1 Procedure

The subject sits 1.5 metres from a monitor, which displays blue/black flickering checkerboards (<6Hz, 10 cd/m2), in rapid sequence in an On-Off mode. Pupils were not dilated and subjects were given appropriate spectacle correction for near vision.

S/He is instructed to fixate the centre of the display. The procedure is repeated after adaptation to yellow light (3 min, 1000 cd/m2) by ColorDome – Diagnosys LLC. The procedure can be paused at any time if necessary.

A black and blue reversing checkerboard stimulus was displayed on a 21-inch Flat Display Premium Color Monitor (Sun microsystems, USA). It covered a field size of 21.6° and the check size was 2.7°. The contrast between black and white squares was greater than 95%. Overall screen luminance did not vary during checkerboard reversals. Frame rate maintained with raster-based CRT of frequency of 75 Hz. Background dim room illumination was used for the entire recordings. A reversal rate of 6 reversals/second (3 Hz) with a sweep time of 150 ms was used. Computerized artifact

rejection was set at 100 μV. Monocular recording was done. 100 responses were averaged. The recording with the least noise was selected, marked and printouts were obtained. The bandpass filters were set at 100 Hz. The timebase was 200ms.
Great care was taken to maintain a constant mean luminance level; thus, any alteration in response amplitude was not confounded by decreases in mean luminance.
A computer program describing the recording parameters was written onto the disc and summoned for each experimental trial. The parameters remained constant within an experimental series. The initial PERG studies incorporated an interrupt button which allowed the subject to control the length of the recording epoch. Volunteers were thus instructed to restrict averaging to between blinks. The following parameters were measured for all subjects: Amplitude and implicit times of P50, P and N95.

2.2.2 Pupillography

Pupil testing was done using the Albomed, a commercially available instrument from Schwarzenbruck, Germany. The pupillary light reflex is measured using infrared technology: An infrared-sensitive CCD-line camera (30 frames/s) detects light emitted by two IR-diodes that is reflected from the iris. The stimulating and recording entity is mounted on a small table with the device and light-source at a distance of 10 cm to the eye. The internal software calculates the left and right margins of the pupil, which is used to measure the pupil dynamics. The test is non-invasive and does not impose any risks for the examined subject.
The Albomed has the ability to provide a variety of full or partial field stimuli to one or both eyes with an LCD screen. While the stimuli are presented, video recording produces a real time pupil diameter that can be analysed at various time points. The patient is seated comfortably with his head on a combined head and chin rest and is instructed to look into the direction of the infrared light source at the lens aperture of the camera. The examination room is as dark as possible. The pupil response to red and blue LED light stimuli respectively of 1s duration at an intensity of 50 lx was recorded for the consensual eye. Four good quality measurements, uncontaminated by artefacts were required for calculation of the mean. Only one eye was examined.

Pupil responses to red and blue light were recorded under both dark (DA) and light (LA) conditions in separate runs. Before testing, the patient was placed in a room for 5 minutes of dark adaptation. The test began with a full field stimulus of red light presented to both eyes for one second. The field would then go dark for 29 seconds, during which the pupil diameter was measured. This period of dark still included the background illumination of the LCD screen. The sequence was then repeated. After the red protocol there was a period of one second of blue light and the test continued as above. This procedure was then repeated for the light adapted conditions after 1min light adaptation.
Baseline pupil diameter was taken to be the average pupil diameter in a dark-adapted eye, over a 1-second period before the light stimulus. The following parameters were measured for all subjects: redilation time(s), maximal constriction (mm) and constriction time(s).

Systolic blood pressure, blood O_2 and pulse were measured before, between and at the end of the recording session to ensure that alterations in these parameters do not contaminate the data (Infinity® Gamma XL Patient Monitor, USA).

2.3 Statistical analysis

All statistical analyses were performed with JMP® statistical software version 13 (SAS Institute, USA); $p < 0.05$ was considered to be statistically significant. Student t test was used to compare the characteristics and results of PERG, and pupillography between glaucoma Patients and healthy subjects. Amplitude values of PERG samples were fitted with a non-linear function and smothing spline lampda 150 function, that minimizes the noise while avoiding assumptions about the relationship among variables. The ratios were compared using Student's t test. Pearson correlation coefficients were calculated between the amplitude of P and the pupillometry measures.
This study follows the tenets of the Declaration of Helsinki for human studies. The study was approved by both the ethical committees of the University of Tübingen (project number 074 / 2017BO2). Written informed consent was obtained from all subjects after the nature of the test and the possible risks were explained in detail.

3. Results

3.1 Subjects

From the 15 control and 15 glaucoma recordings, 5 of each produced PERG curves that were too noisy to be analysed. Therefore, a total of 10 eyes of glaucoma subjects and 10 eyes of healthy subjects were included in this study.

In Table 1, the subjects' clinical characteristics are listed. The mean age of the healthy subjects was 31.2 yrs (+/-10SD), that of the glaucoma group 61.0 yrs (+/-15.2SD). There were 3 females in the healthy group and 4 in the glaucoma group. The average ocular tension was similar in both groups (16.2, 16.1 respectively), but the standard deviation was much larger in the glaucoma group (3.8) than the healthy controls (0.78).

Table 1 Summary of subjects' clinical characteristics

Patient number	Patient group	Gender	Age (yr)	Visual acuity	Ocular tension (mm Hg)
1	h	f	47	1.0	16
2	h	m	28	1.0	17
3	h	f	26	1.0	15
4	h	m	49	1.0	16
5	h	f	20	1.0	17
6	h	m	33	1.0	17
7	h	m	25	1.0	15
8	h	m	21	1.0	16
9	h	m	35	1.0	17
10	h	m	28	1.0	16
1	g	m	39	0.8	16
2	g	f	70	1.0	18
3	g	m	78	0,6	16
4	g	f	66	1.0	10
5	g	m	52	0,8	19
6	g	f	75	0.9	20
7	g	m	58	1.25	12
8	g	f	50	1.0	22
9	g	m	41	1.0	16
10	g	m	81	0.6	12

Abbreviations: m: male, f: female, h: healthy subjects, g: glaucoma patients.

3.2 PERG

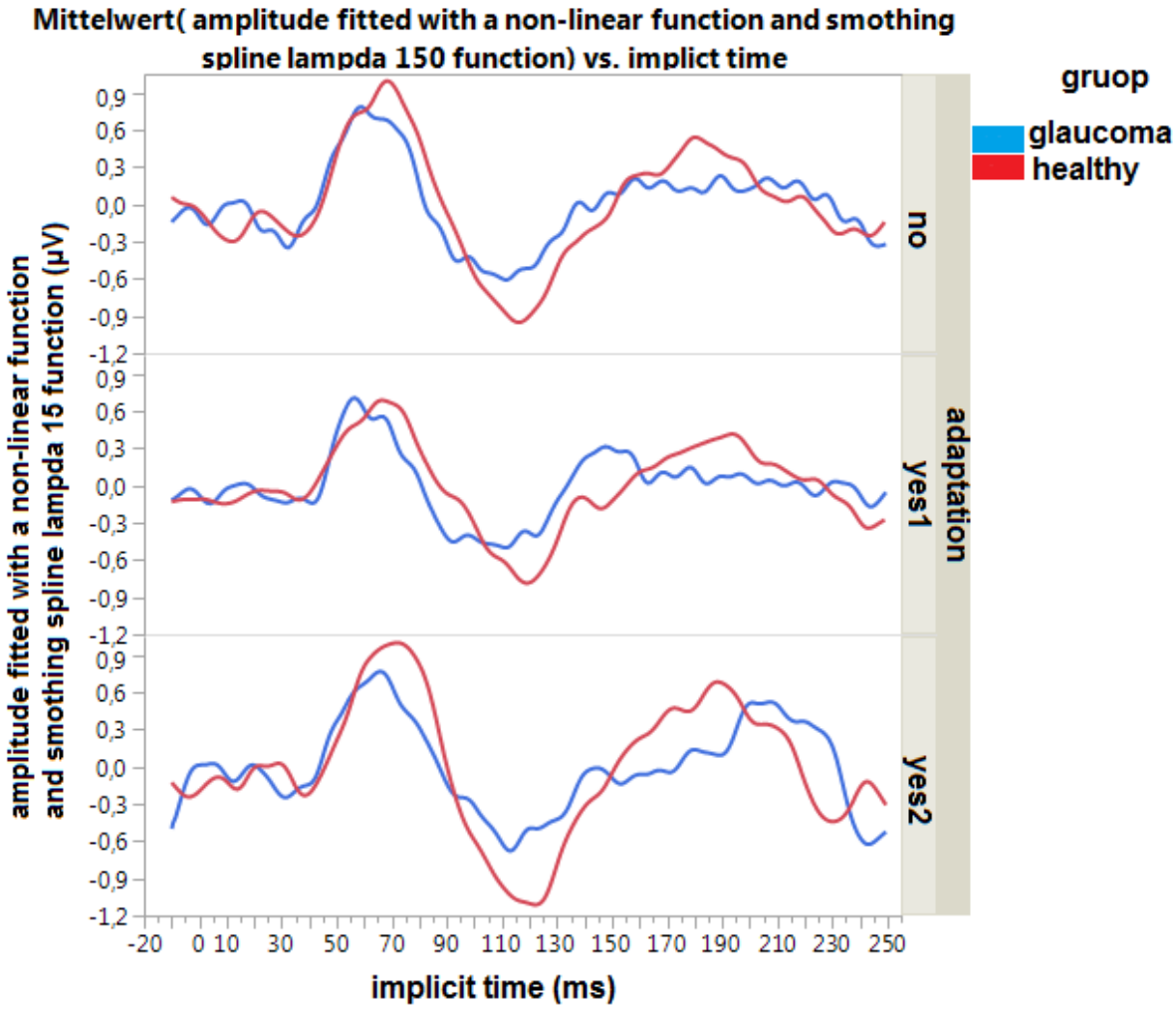

Figure 8 Average PERGs recorded from healthy controls (red lines) and glaucoma patients (blue lines). The upper panel shows the results before adaptation to a yellow background (no) whereas the central and lower panels show the results after 1 min (yes1) and after 2min (yes2) yellow adaptation, respectively.

In Fig. 8 the mean transient PERG recorded from healthy controls (red lines) and glaucoma patients (blue lines) is depicted. It will be seen that the amplitude of P50 and

N95 tend to be smaller for glaucoma patients and earlier, but the small S-cone peak P is not visible. This is because the mean value from PERG recordings is not an accurate parameter as smaller peaks and troughs can cancel each other out if they don't have the same implicit times. For further analysis therefore we used the individual peak times of each subject to calculate the average responses and significance. The results for each subject are given in the Tables 2 and 3.

Table 2 Individual PERGs' results from healthy subjects.

Subject number	**1**	**2**	**3**	**4**	**5**	**6**	**7**	**8**	**9**	**10**
eye	OD	OD	OD	OS	OS	OD	OD	OD	OS	OS
Amp P50 no	1.73	2.32	2.92	0.9	2.52	2.81	1.11	1.98	1.55	2.19
Amp P50 yes1	1.66	1.42	1.37	1.01	2.17	2.21	1.25	1.19	0.63	3.42
Amp P50 yes2	2.44	3.3	2.33	0.64	2.15	2.31	0.89	1.54	0.53	2.03
Imp P50 no	68	72	55	59	65.5	62.5	67	68.5	51	66.5
Imp P50 yes1	70	66.5	65.5	69	60	61.5	75	71	52	73.5
Imp P50 yes2	74.5	74	60.5	58.	61.5	72.5	77	67	57.5	64
P Amp yes1	1.61	2.11	1.19	0.63	0.54	2.58	0.77	1.31	0.21	2.36
P Amp yes2	2.61	2.2	1.36	0.05	1.13	0.2	0.5	0.4	0.35	0.99
P Imp yes1	86	85	90.5	92.5	2.71	94	93.5	91.5	91	92
P Imp yes2	95	85.5	75	84	1.02	84.5	85	81.5	79	75
N95 Amp no	2.44	1.77	4.14	0.82	-3.9	4.14	1.12	2.29	2.17	-2.7
N95 Amp yes1	2.38	2.61	2.49	1.06	4.14	3.18	1.24	2.14	0.65	-1.7
N95 Amp yes2	2.13	-4.4	3.43	-1.4	3.28	6.38	0.86	2.22	0.47	2.42

Abbreviations: PERG: pattern electroretinogram, N: number of subjects, m: male, f: female, Amp: amplitude, Imp: implicit time, no: without yellow adaptation, yes1: is the PERG measure 1 minute after yellow light adaptation, yes2: is the PERG measure after 2 minutes of yellow adaptation.

Table 3 Individual PERGs' results from glaucoma patients

Subject number	1	2	3	4	5	6	7	8	9	10
Gender	m	f	m	f	m	f	m	f	m	m
eye	OD	OS	OS	OS	OS	OD	OD	OD	OS	OS
Amp P50 no	2.31	1.28	1.59	1.47	2.78	1.7	2.53	1.68	1.41	0.83
Amp P50 yes1	2.25	1.36	1.12	1.09	0.46	0.91	1.59	1.15	2.04	0.39
Amp P50 yes2	4.39	1.51	0.73	1.25	2.45	1.05	0.67	1.78	2.07	0.39
Imp P50 no	67	45.5	52.5	48.5	54	57.5	55.5	67	58	58
Imp P50 yes1	68	53.	46	55	61	55	64.5	65	57	51.5
Imp P50 yes2	76	61.5	52.	52.5	55	53	62.5	54	56	39.5
P Amp yes1	2.17	0.88	0.73	0.8	0.29	0.58	1.23	-0.42	1.02	0.19
P Amp yes2	2.64	1.04	0.34	0.59	1.06	0.24	-0.02	1.35	0.65	0.18
P Imp yes1	86	77	57.5	77	62.5	68.5	79	78	74	64
P Imp yes2	92	78	68	64	74.5	66.5	87	72.5	65	60.5
N95 Amp no	2.19	-1.13	-1.79	-1.79	-4.37	-2.07	-2.4	-2.33	-1.24	-1.26
N95 Amp yes1	0.71	-2.12	-1.1	-2.28	-1.28	-1	-2.76	-1.12	-2.49	-0.58
N95 Amp yes2	-2.3	-1.53	-1.3	-2.11	-3.97	-1.88	-1.39	-1.09	-2.75	-0.72

Abbreviations: PERG: pattern electroretinogram, N: number of subject, m: male, f: female, Amp: amplitude, Imp: implicit time, no: without yellow adaptation, yes1: is the PERG measure 1 minute after yellow light adaptation, yes2: is the PERG measure after 2 minutes of yellow adaptation.

The averages thus calculated are depicted in the histograms in Fig. 9 and listed in Table 4.

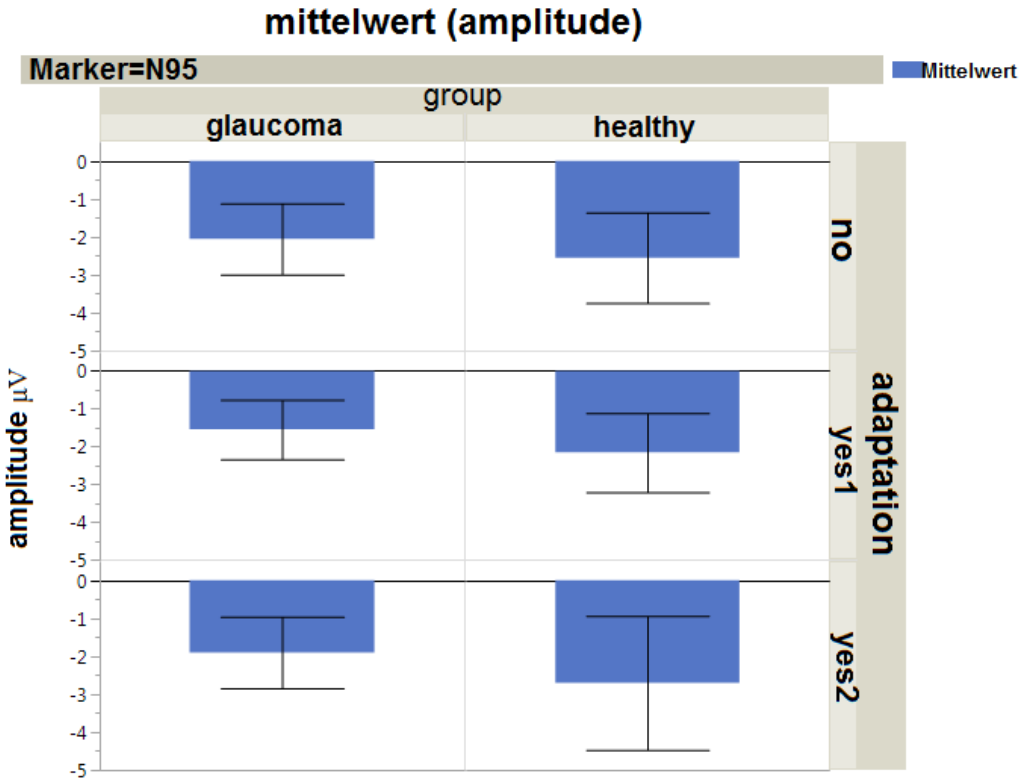
mittelwert (amplitude)
Marker=N95
Mittelwert
group
glaucoma
healthy
amplitude µV
adaptation
no
yes1
yes2
0
-1
-2
-3
-4
-5

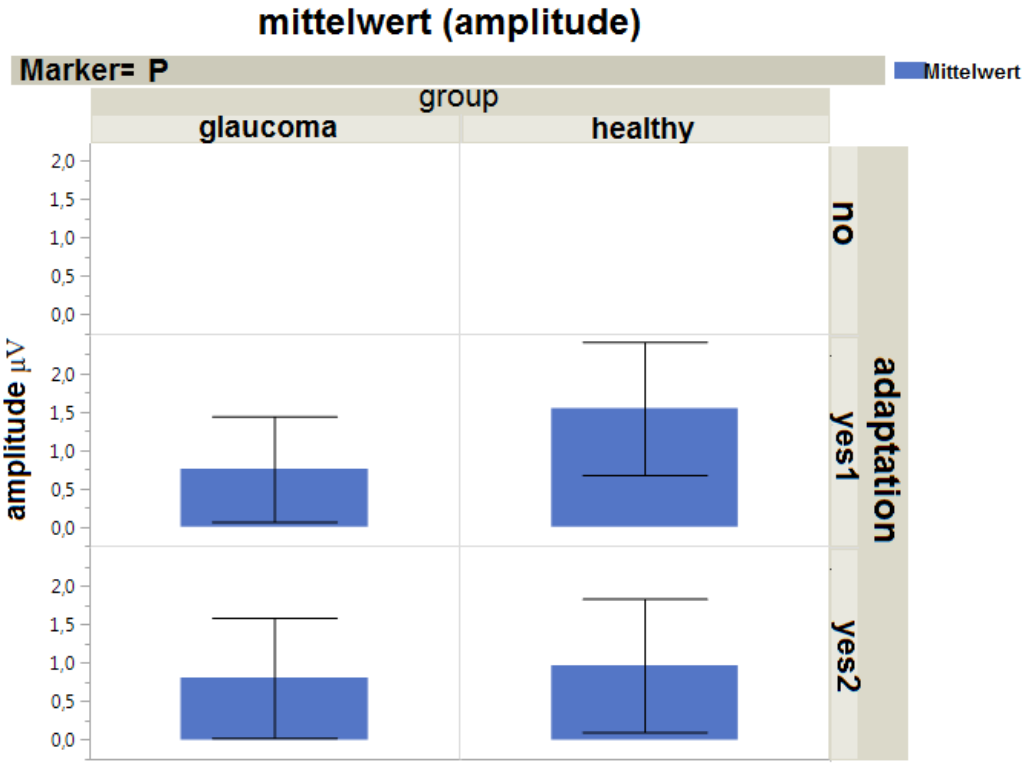
mittelwert (amplitude)
Marker= P
Mittelwert
group
glaucoma
healthy
amplitude µV
adaptation
no
yes1
yes2
2,0
1,5
1,0
0,5
0,0

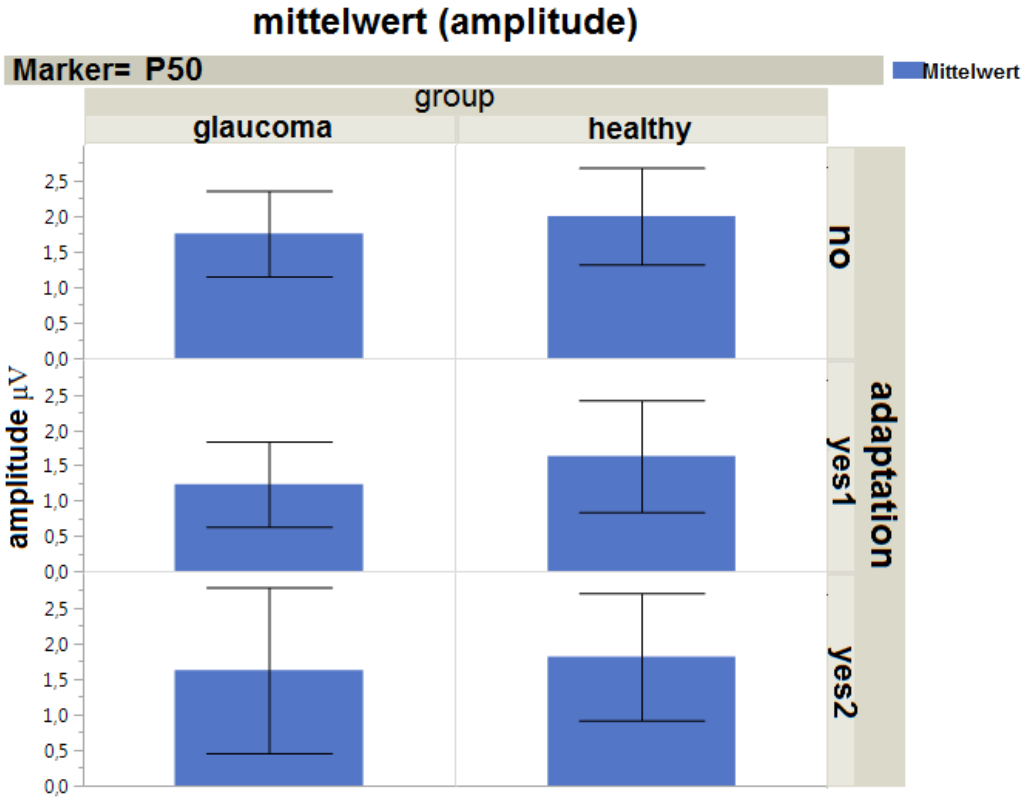
mittelwert (amplitude)
Marker= P50
Mittelwert
group
glaucoma
healthy
amplitude µV
2,5
2,0
1,5
1,0
0,5
0,0
no
yes1
yes2
adaptation

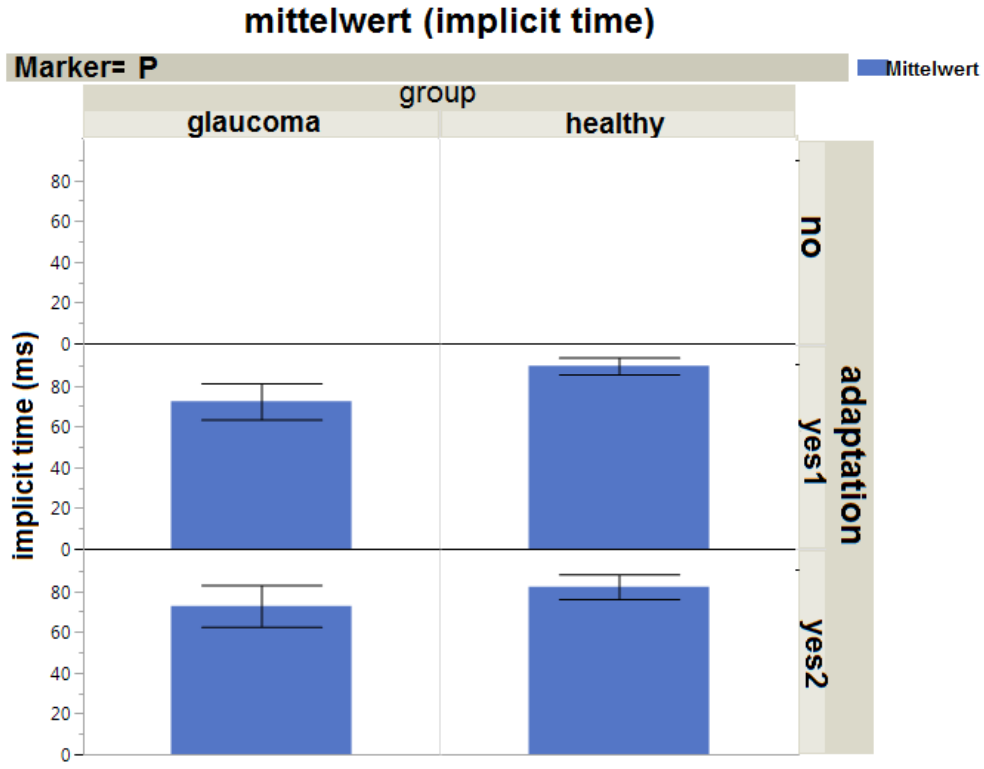
mittelwert (implicit time)
Marker= P
Mittelwert
group
glaucoma
healthy
implicit time (ms)
80
60
40
20
0
no
yes1
yes2
adaptation

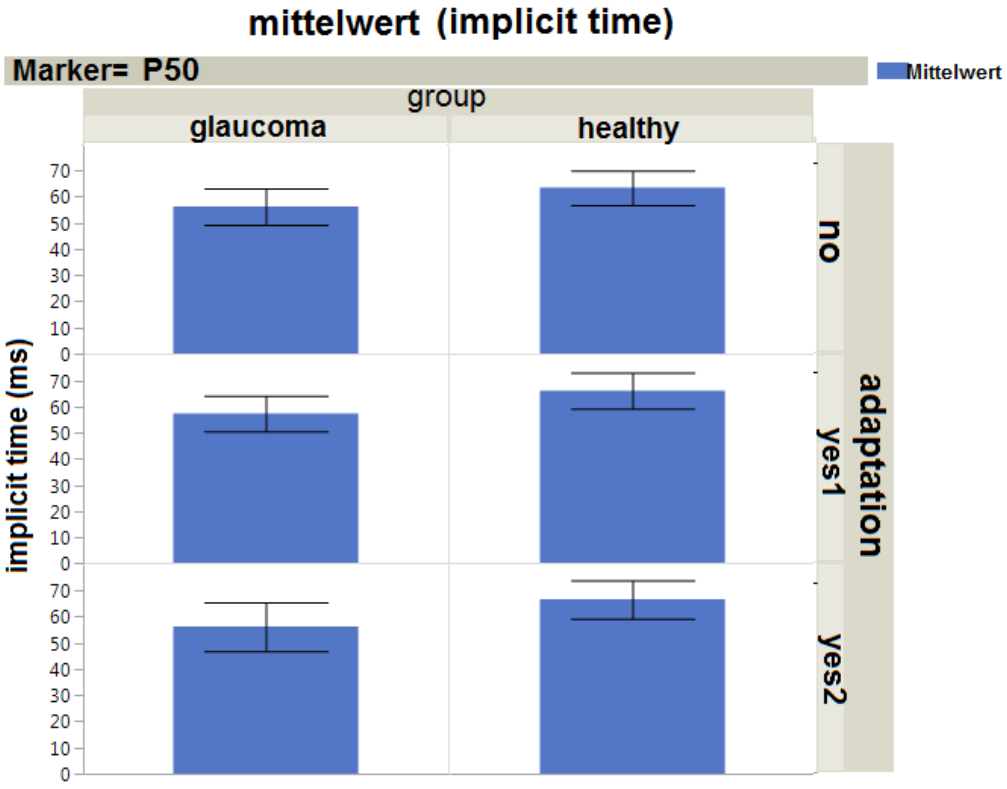

Figure 9 average amplitudes of the PERG (N95, P and P50); average implicit times of the PERG (P and P50) (No = measurement of PERG with no previous yellow adaptation, Yes1 = measurement of PERG after 1 minute of yellow adaptation, Yes2 = measurement of PERG after 1 minute of yellow adaptation.)

Table 4 Comparison of PERG parameters between subject groups

Pattern ERG parameter	Glaucoma patients	Healthy subjects	*p-value**
P50 amplitude, μV (before yellow adaptation)	1.758 (±0.60)	2.003 (±0.68)	0.203
P50 amplitude, μV (after 1 minute of yellow adaptation)	1.236 (±0.60)	1.633 (±0.79)	0.112
P50 amplitude, μV (after 2 minutes of yellow adaptation)	1.629 (±1.16)	1.816 (±0.89)	0.346
P50 implicit time, ms (before yellow adaptation)	56.35 (±6.94)	63.5(±6.60)	**0.014**
P50 implicit time, ms (after 1 minute of yellow adaptation)	57.65 (±6.86)	66.4 (±6.97)	**0.005**
P50 implicit time, ms (after 2 minutes of yellow adaptation)	56.25(±9.32)	66.7 (±7.29)	**0.006**
P amplitude, μV (after 1 minute of yellow adaptation)	0.755 (±0.68)	1.548 (±0.87)	**0.018**
P amplitude, μV (after 2 minutes of yellow adaptation)	0.807 (±0.77)	0.968 (±0.86)	0.333
P implicit time, ms (after 1 minute of yellow adaptation)	72.35 (±8.88)	89.75 (±4.14)	4.225
P implicit time, ms (after 2 minutes of yellow adaptation)	72.8 (±10.2)	82.2 (±6.03)	**0.012**
N95 amplitude, μV (before yellow adaptation)	-2.057 (±0.93)	-2.549 (±1.19)	0.159
N95 amplitude, μV (after 1 minute of yellow adaptation)	-1.546 (±0.78)	-2.159 (±1.04)	0.078
N95 amplitude, μV (after 2 minutes of yellow adaptation)	-1.904 (±0.94)	-2.699 (±1.76)	0.114

* The probability *p* of the results occurring by chance. Bold values are significant at *p*=0.05. Correction for multiple testing would set *p* to be significant at 0.004 and not 0.05 (see Discussion).

From Table 4 and Figure 9 it will be seen that the mean amplitude values for P50 in the glaucoma patients was 1.758 (±0.60) uV before yellow light adaptation, 1.236 (±0.60) uV after the first minute with yellow light adaptation and 1.629 (±1.16) uV after the second, whereas the mean amplitude values for P50 in the healthy subjects were higher: 2.003 (±0.68) uV before yellow light adaptation, 1.633 (±0.79) uV after the first minute adaptation and 1.816 (±0.89) uV after the second minute of yellow light adaptation. No

significant differences in these mean values of amplitude were found. On the other hand, there were significant differences between the 2 groups for the implicit times for all 3 parameters: The mean implicit time for P50 in the glaucoma patients was 56.35 (±6.94) ms before yellow light adaptation, 57.65 (±6.86) ms after one minute of yellow light adaptation and 56.25(±9.32) ms after 2 min adaptation, whereas the mean implicit time values for P50 in the healthy subjects were longer: 63.5 (±6.60) ms before yellow light adaptation, 66.4 (±6.97) ms after 1 min of yellow light adaptation and 66.7 (±7.29) ms after 2 min (*p* values were: 0.014, 0.005 and 0.006 respectively).

The mean values for the P (S-cone) amplitude in the glaucoma patients were 0.755 (±0.68) uV after the first PERG measurement with 1 min of yellow light adaptation and 0.807 (±0.77) uV after the second, whereas the mean amplitude values for P in the healthy subjects were 1.548 (±0.87) uV after 1 min of yellow light adaptation and 0.968 (±0.86) uV after 2 min. Thereby it must be remembered that a small value of P indicates a larger peak, because the amplitude was measured from the P50 peak. A significant difference between healthy and glaucoma patients was found only for the P amplitude after the first PERG measure with yellow light adaptation ($p = 0.018$). Implicit times were also significantly longer 2 min after adaptation.

Also to be seen in Table 4 and Fig. 9 are the N95 amplitudes. The mean amplitude values for N95 in the glaucoma patients were -2.057 (±0.93) uV, -1.546 (±0.78) uV, and -1.904 (±0.94) uV before, after 1min and after 2 min yellow light adaptation respectively. The mean amplitude values for N95 in the healthy subjects were higher: -2.549 (±1.19) uV, -2.159 (±1.04) uV and -2.699 (±1.76) uV) but the differences were not significant.

3.3 Pupillometry

In Fig. 10, a representative PIPR response from a healthy subject is shown to a red and blue stimulus under dark - (upper panels) and light adapted (lower panels) conditions. It will be seen that the redilation time to a blue stimulus under light adaptation is longer than under dark adaptation. The results for each subject are shown in Table 5.

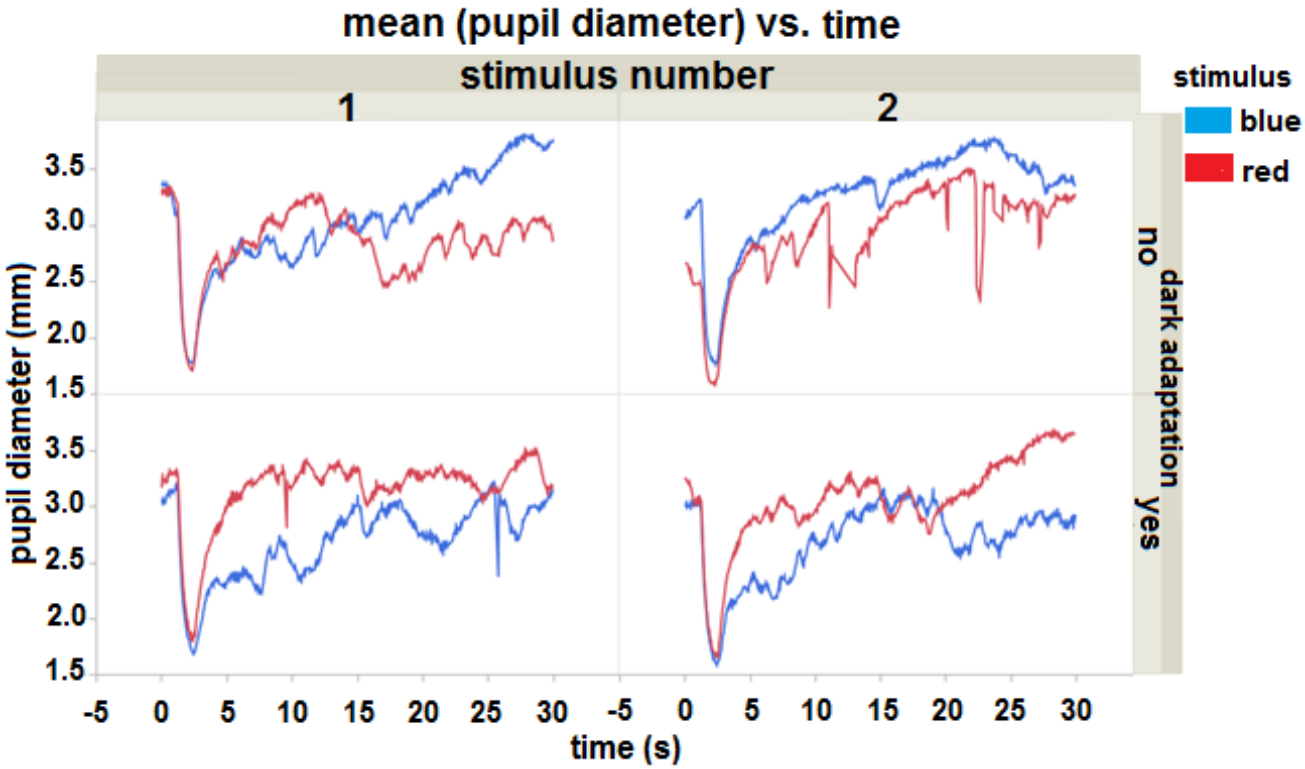

Figure 10 PLR responses to a red (red lines) and blue (blue lines) stimulus from a healthy subject under dark-(upper panels) and light adapted (lower panels) conditions. Results from 2 runs (1, 2,)

Table 5 Individual results for pupillometry parameters

			CT	**MC**	**RT**	**CT**	**MC**	**RT**	**CT**	**MC**	**RT**	**CT**	**MC**	**RT**
N	eye	G	Blue LA			Blue DA			Red LA			Red DA		
1	OD	h	2.5	3.30	25.96	2.66	3.84	29.97	2.43	3.75	25.26	2.4	3.34	29.96
2	OD	h	2.66	4.65	29.97	2.5	4.2	29.97	2.56	4.54	29.96	2.4	2.79	24.3
3	OD	h	2.46	2.86	29.97	2.167	2.81	26.57	2.5	3.24	25.43	2.37	1.81	27.63
4	OS	h	2.37	1.75	20.46	2.5	1.66	24.57	2.43	3.28	24.23	2.43	1.82	18.2
5	OS	h	2.67	3.39	17.6	2.77	3.11	28.4	2.33	1.73	29.97	2.43	3.53	15
6	OD	h	2.3	3.41	19.27	2.6	3.31	29.97	2.3	3.51	24.03	2.5	3.99	15.57
7	OD	h	3	3.29	29.97	2.97	3.55	29.97	2.63	3.91	29.97	2.47	3.45	15.53
8	OD	h	2.97	2.07	28.67	2.37	2.684	24.97	2.5	3.15	26.23	2.5	2.68	26.83
9	OS	h	2.53	2.73	27.67	2.467	2.66	28.3	2.533	3.29	26.17	2.5	2.90	21.2
10	OS	h	3.23	3.73	19.77	2.4	3.55	24.77	2.6	3.24	25.9	2.3	3.82	18.4
1	OD	g	2.33	2.58	29.3	2.3	2.45	18.36	2.33	2.56	29.96	2.36	2.46	29.96
2	OS	g	2.53	3.86	29.3	2.47	3.163	12.53	2.53	3.68	18.3	2.53	3.26	26.56
3	OS	g	2.4	2.67	24.46	2.4	2.403	16.66	2.36	2.68	18.66	2.36	2.51	14.6
4	OS	g	4.63	2.67	24.86	1.7	3.49	18.26	2.43	3.56	14.46	2.5	3.52	13.36
5	OS	g	2.4	4.76	29.97	2.4	4.754	19.1	2.4	4.45	18.13	2.367	4.73	29.96
6	OD	g	2.37	2.82	29.97	2.16	2.86	15.47	2.36	2.74	24.8	2.3	2.84	29.96
7	OD	g	1.97	4.36	24.6	1.3	5.01	29.97	2.03	2.67	13.57	2.5	5.75	10.33
8	OD	g	2.57	2.37	29.67	2.167	2.71	16.9	2.37	2.46	18.43	2.37	2.4	13.97
9	OS	g	2.7	2.33	32.33	2.633	2.06	13.77	2.43	2.49	13.93	1.43	1.72	10.8
10	OS	g	1.97	4.75	29.97	2.13	5.46	29.97	1.5	2.145	15.8	2.5	6.0	14.03

Abbreviations: N: number of subject, Gr: group, h: healthy subjects, g: glaucoma patients, CT: constriction time of the Pupil after Light stimulus, MC: maximal constriction of the pupil after light stimulus, RT: redilation time of the pupil after light stimulus, blue LA is the pupillography measure after blue stimulus with light adaptation, blue DA is the pupillography measure after blue stimulus with dark adaptation, red LA is the pupillography measure after red stimulus with light adaptation, red DA is the pupillography measure after red stimulus with dark adaptation

In Table 6 the average of the pupillography parameters are listed.

Table 6 Mean pupillography results of the study participants

Pupillometry parameter	**Glaucoma patents**	**Healthy subjects**	***p*-value***
constriction time ms (blue LA)	2.57 (±0.719)	2.67 (±0.303)	0.343
maximal constriction mm (blue LA)	3.29(±0.953)	3.11 (±0.825)	0.323
redilation time ms (blue LA)	28.16 (±2.771)	24.93 (±5.066)	**0.047**
constriction time ms (blue DA)	2.20 (±0.390)	2.54(±0.223)	**0.012**
maximal constriction mm (blue DA)	3.38 (±1.161)	3.13(±0.724)	0.279
redilation time ms (blue DA)	19.99 (±6.487)	27.74(±2.322)	**0.001**
constriction time ms (red LA)	2.29 (±0.294)	2.48(±0.109)	**0.036**
maximal constriction mm (blue DA)	3.01 (±0.717)	3.35(±0.717)	0.144
redilation time ms (red LA)	19.60(±5.909)	26.71(±2.357)	1.113
constriction time ms (red DA)	2.34(±0.312)	2.43(±0.065)	0.192
maximal constriction mm (red DA)	3.49(±1.407)	3.01(±0.761)	0.168
redilation time ms (red DA)	20.32(±8.732)	21.2(±5.564)	0.384

Abbreviations: blue LA: pupillography measure after a blue stimulus with previous light adaptation, blue DA: after a blue stimulus with previous dark adaptation, red LA: after a red stimulus with light adaptation, red DA: after a red stimulus with dark adaptation. * as for Table 2.

Significant differences in pupil parameters between healthy controls and glaucoma patients: were found with a blue stimulus for the redilation times after both light (p = 0.047) and dark adaptation (p = 0.001), as well as for the constriction time after dark adaptation (p = 0.012). With a red stimulus only the constriction time with light adaptation was significant (p = 0.036). The maximal constriction time was not significant between subject groups for all parameters. The results are depicted in the histograms below.

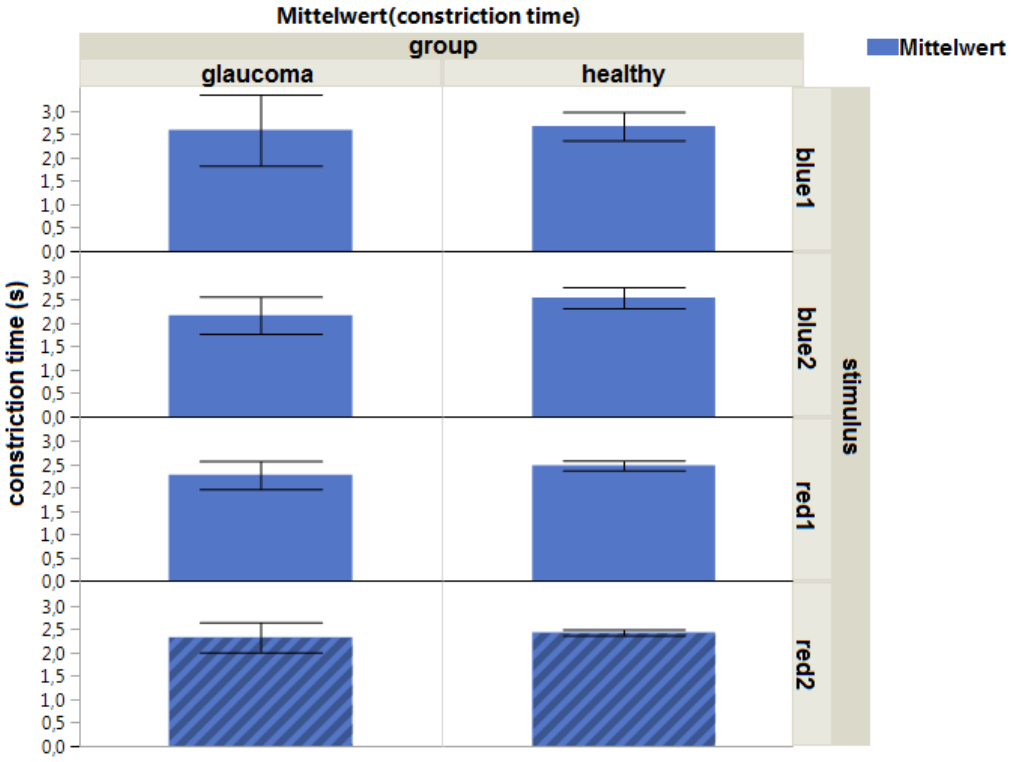
Mittelwert(constriction time)
group
glaucoma
healthy
Mittelwert
constriction time (s)
stimulus
blue1
blue2
red1
red2
0,0
0,5
1,0
1,5
2,0
2,5
3,0

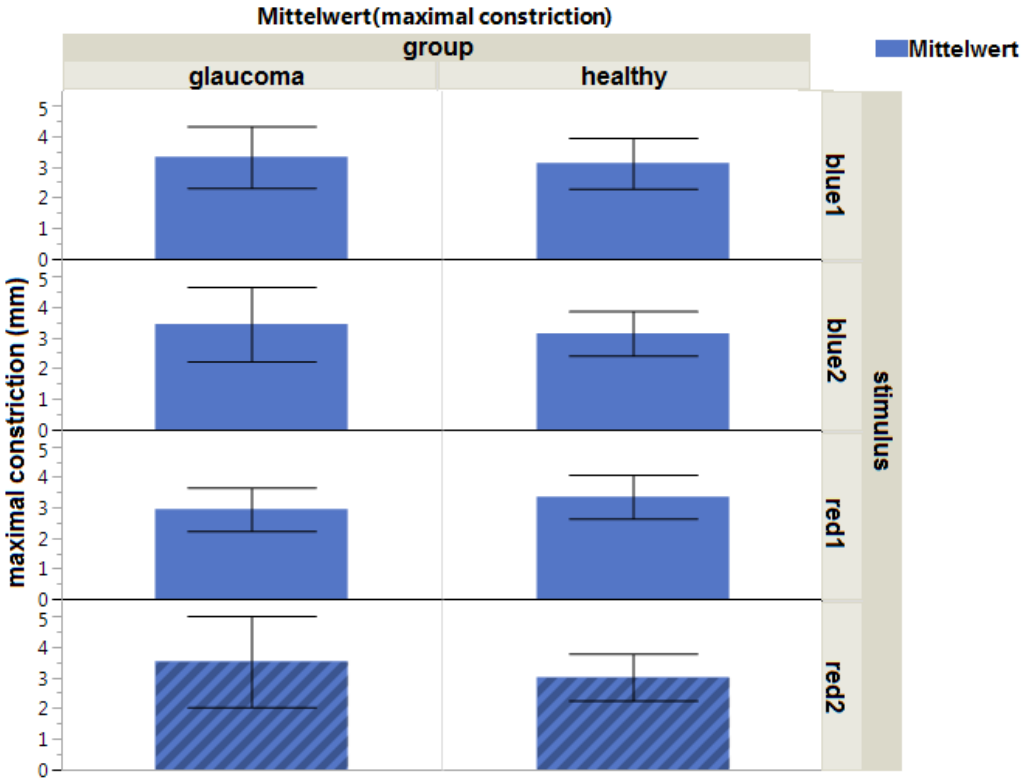
Mittelwert(maximal constriction)
group
glaucoma
healthy
Mittelwert
maximal constriction (mm)
stimulus
blue1
blue2
red1
red2
0
1
2
3
4
5

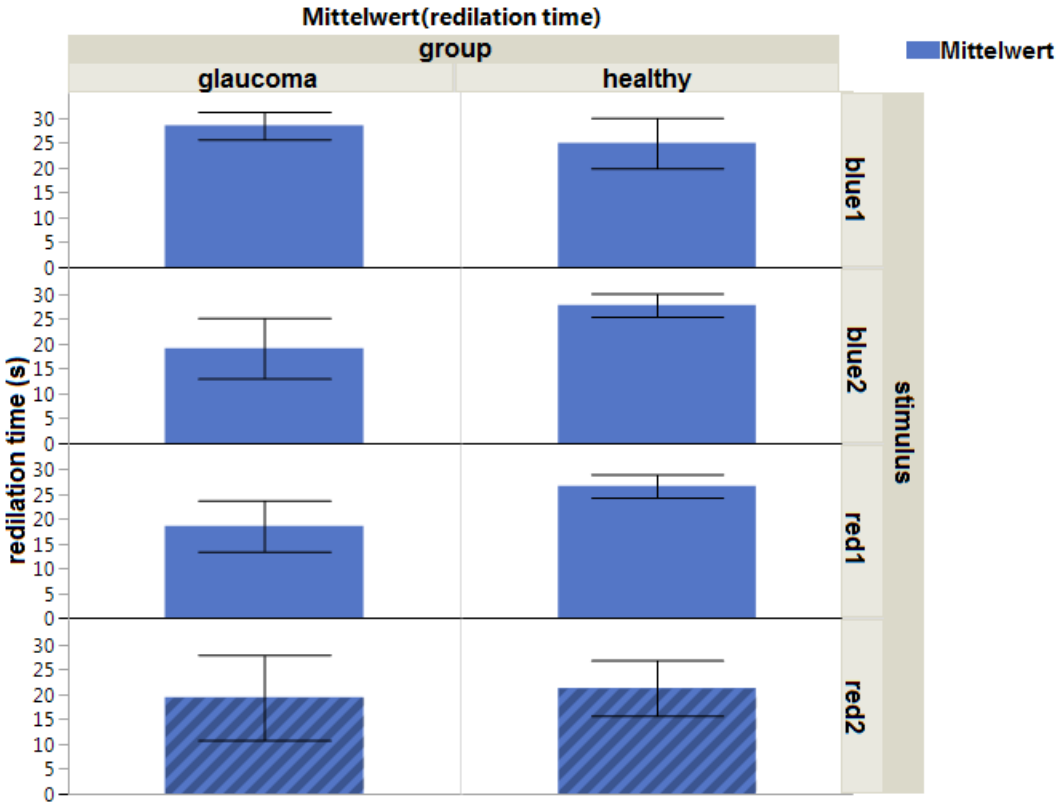

Figure 11: Pupillometry: Average +/- SD of of constriction time, maximal constriction and redilation time. *Upper panels:* (blue1) blue light stimulus with light adaptation; *second upper*: (blue 2 blue stimulus with dark adaptation; *second lower panels:* (red 1) red stimulus with light adaptation and *lower panels:* (red 2) red stimulus with dark adaptation.

3.4 Comparison between S-cone activity from the PERG and pupil ipRGCs

To compare S-cone activity from the PERG and the pupil responses, we calculated the Pearson correlation coefficients between their parameters. These are listed in Table 7.

Table 7 Correlation coefficients (CC) between the amplitude P (S-cone) of the PERG and the redilation time from pupillography.

Redilation time parameter from PIPR subject group: recording condition	Correlation coefficient (CC) with amplitude P (S-cone)
healthy: 1 min after adaptation, blue LA	**-0.550**
healthy: 1 min after adaptation, blue DA	0.195
healthy: 1 min after adaptation, red LA	0.170
healthy: 1 min after adaptation, red DA	-0.217
glaucoma: 1 min after adaptation, blue LA	-0.181
glaucoma: 1 min after adaptation, blue DA	-0.028
glaucoma: 1 min after adaptation, red LA	0.399
glaucoma: 1 min after adaptation, time red DA	0.212
healthy: 2 min after adaptation, blue LA	0.295
healthy: 2 min after adaptation, blue DA	0.403
healthy: 2 min after adaptation, blue LA	0.256
healthy: 2 min after adaptation, blueDA	**0.620**
glaucoma: 2 min after adaptation, blue LA	0.320
glaucoma: 2 min after adaptation, blue DA	-0.367
glaucoma: 2 min after adaptation, red LA	**0.678**
glaucoma: 2 min after adaptation, red DA	**0.508**

Abbreviations DA: dark-adapted; LA: light adapted

A CC of 1 (or -1) indicates a strong positive (or negative) linear relationship, a CC of 0 indicates no linear relationship. The results show no strong correlations. A moderate negative relationship for the correlation between P and the redilation time in the healthy group in the first minute of adaptation in the light adapted condition with a blue/black stimulus (CC= -0.550). Moderate positive correlations were also found in the healthy

group with a blue stimulus 2 min after DA (0.620), and in the glaucoma 2 min after adaptation for not a red and blue stimulus **(**0.678, 0.508 respectively).

3.5 Blood pressure, pulse and oxygen

In Table 5 we list the mean blood pressure, pulse and oxygen measurements made at the beginning (1), during (2) and at the end (3) of the experimental session,

Table 8: Blood pressure pulse and oxygen

	glaucoma (n = 10)	**healthy (n = 10)**	***p* value**
Average BP1	137.1 (±15.94)	120.6 (±13.36)	**0.011**
Average BP2	132.9 (±15.22)	122.2 (±11.29)	**0.046**
Average BP3	132.7 (±14.079)	122.9 (±12.47)	0.058
Pulse 1	90.83 (±6.93)	74.1 (±3.107)	0.261
Pulse 2	69.5 (±9.721)	73 (±4.898)	0.163
Pulse 3	70 (±8.993)	73.4 (±4.0879)	0.148
Average O^2-1	98.4 (±1.505)	98.3 (±0.948)	0.430
Average O^2-2	97.7 (±1.7669)	98.3 (±0.823)	0.174
Average O^2-3	98 (±1.490)	98.5 (±0.849)	0.186

Abbreviations: BP1, Puls1, O2-1: systolic blood pressure, pulse and blood oxygen saturation: first measure before PERG, BP2, Puls2, O2-2: second measure after PERG, BP3, Puls3, O2-3: third measure after pupillography.

The systolic blood pressure was significantly higher in the glaucoma patients before and after the PERG recording, but the oxygen saturation and the pulse showed no significant differences between glaucoma subjects and the healthy control group.

4. Discussion

The aim of this study was to ascertain whether the relatively recently discovered ipRGCs in the retinal ganglion cell layer can be detected in electrophysiological recordings of retinal activity. We examined the transient PERG, which has been shown to arise specifically in the RGC layer (Bach et al., 2018), under conditions favouring the short wavelengths to which melanopsin is sensitive and correlated the S-cone amplitude with recordings of the pupil response to blue light where melanopsin has been shown to be active. The hypothesis was that if melanopsin contributes to the PERG it will contribute to amplitude of P (S-cone), because of the similarity in their spectral sensitivities.

The results of the PERG recordings showed significantly early P50 amplitudes in the glaucoma patients. Amplitudes were also reduced, but not significantly (Fig. 8, Table 2). Glaucoma is a progressive optic neuropathy that is accompanied by injury to retinal ganglion cell axons and also other tissues of the optic nerve (Porciatti et al., 2015). Many studies have shown that the PERG largely stems from the retinal ganglion cells. The major peak, P50 and major trough N95 reflect retinal ganglion cell function, but there is an additional more distal retinal contribution to the P50 component. In severe or chronic retinal ganglion cell dysfunction, there may be P50 reduction, but P50 also usually shortens in implicit time, as we find, which reflects the loss of the retinal ganglion cell contribution to P50.

It has been shown that PERG can identify changes in RGC function at an early stage and even before the onset of the thinning of the retinal neurons (Cvenkel et al., 2017). A significant correlation between PERG amplitudes and disc morphology in glaucoma suspect has also been shown. In early glaucoma or suspected glaucoma, the correlation between RNFL thickness and the N95 wave of the PERG is significant, whereas the P50 wave of PERG showed no significant correlation (Jeon et al., 2019). Another study concluded that we might be able to identify the early glaucomatous damage by examining from the PERG (Jung et al., 2020). The PERG can thus show disturbances in ganglion cell function before they die (Jeon et al., 2019). A further study has shown that the amplitude of the PERG in glaucoma suspects gradually decreases over time. This decrease shows no significant correlation with retinal fibre layer progression, but the

progression of both PERG and retinal fibre layer continue with the further progression of the visual field (Gordon et al., 2020).

Although the transient PERG can identify the glaucomatous alterations in RGCs, they cannot be used reliably for the early detection of glaucoma or for monitoring disease progression. In a clinical setting, the usual routine topographical examinations for monitoring the progression of glaucoma are still better, more reliable and more practical (Senger et al., 2020). A few studies have shown that patients with glaucoma have an abnormal pupillary light reflex (RAPD), and it likely suggests damage to the optic nerve system (Wilhelm & Wilhelm, 2003).

The pupillography results also found differences between the glaucoma patients and the healthy controls, especially in the redilation time (Table 3). This confirms reports that the patients with glaucoma have a prolonged redilation time of pupillary reaction after photopic stimulus (Kankipati et al., 2011). This has increased the role of chromatic pupillography in this field, which with the use of blue or red light stimuli can give an assessment of the integrity of the ipRGCs and outer retinal photoreceptors (Rukmini et al., 2019). The study has shown that PIPR decreased relatively more in glaucoma patients after a blue stimulus compared with PIPR after a red stimulus. This indicates reduced light transmission from the ipRGCs (Rukmini et al., 2019).

Some studies have discussed the possibility of early diagnosis of glaucoma with the help of pupillography. But there are many factors that could influence the accuracy of the pupillography parameters, for example the previous ocular surgery, eye drops, and irregular pupil shape, therefore the preliminary examinations and the prehistory are indispensably important (Tatham et al., 2014).

In the PERG recordings to blue-black checkerboards after yellow light adaptation, there was some evidence of a small peak (P) after the P50 peak with an implicit time between 90-110 ms. This has been reported as being the S-cone response (Niepel & Dodt, 1989) which was found in the majority of the curves, but not all.
Because the P amplitude was measured from the P50 peak and not the baseline, large values indicate a small amplitude. Thus we find a smaller P amplitude in healthy subjects

than in glaucoma patients. P was larger after 1 minute of yellow adaptation than after 2 minutes of yellow adaptation in healthy subjects, as expected, but there was no difference in glaucoma patients. In addition, the P amplitude after yellow light adaptation showed a difference between the healthy and the glaucoma group: The P amplitude was significantly larger in the glaucoma group, than in the healthy subjects. This may indicate involvement of the light-sensitive function of the ipRGCs in the function of the S-cone, which is reduced in glaucoma patients because of the impairment of the ipRGC function. This light-sensitive function of ipRGCs may have a passive influence on the light-sensitive function of the S-cone. It is possible that the ipRGCs inhibit the light-sensitive function of the S-cone.

In the glaucoma group there was initially a significant positive correlation between the P amplitude of the PERG after 2 min of yellow light adaptation and the redilation time of the pupil after red stimulation with dark adaptation as well as with light adaptation. In contrast, in healthy subjects, a negative correlation was found between the P amplitude of the PERG after 1 min of yellow light adaptation and the redilation time of the pupil after blue stimulation with light adaptation. This supports the theory of a possible influence of the healthy ipRGCs on the S-cone, which means a possible prolonging of the redilation time of the pupil after activation of the ipRGCs by the blue stimulus. In addition, we found that the redilation time of the pupil was longer in the healthy group than in the glaucoma group, except for the recordings with a blue stimulus under light adaptation. This confirms the known influence of ipRGCs on the regulation of pupillary function. The latter result reinforces the assumption that ipRGCs have an indirect involvement with the P amplitude which is probably derived from the S-cone.

Before, during and after testing, systolic blood pressure, pulse and blood oxygen were measured. There are reports about the influence of systemic blood pressure on retinal sensitivity in human subjects (Henkes et al., 1954, Bellini et al., 1995, Kergoat & Forcier, 1996). We therefore measured systolic blood pressure, pulse and blood oxygen, before, during and after testing, to ensure that these parameters do not influence the results. The results (Table 8), do show a significant difference between subject groups for blood pressure, but the difference is too small to be of consequence.

This study could not confirm the activity of ipRGCs in transient PERG recordings of ganglion cell activity, but there are several limitations. The low amplitudes of PERG and the extremely small P (S-cone) peak, make the study difficult and leads to large variances in the data. A second limitation lies in the subject population tested. Due to the low amplitudes of the PERG, some subjects had to be excluded, so that only the results of 10 healthy and 10 glaucoma patients could be analysed. Further, there is an age difference between the 2 populations which could lead to exaggerated differences between the 2 populations, as the amplitudes of the PERG decrease with age. Furthermore, we cannot ignore that PERGs are attenuated by some factors such as poor refraction, ocular media opacity and macular dysfunction, although these factors were controlled for in the anamnese. Finally, the statistical analysis did not correct for multiple testing, because the limitations listed above made it necessary to favour a higher sensitivity for possible statistically significant differences.

The conclusion is tentative and further study is required to provide more information about the use of the PERG to measure the activity of the ipRGCs. Larger studies are necessary, to confirm the P peak as an additional special component of PERG and to correlate pupillary function of the ipRGCs with P amplitude. Here also comes the question of whether ipRGCs could have other unknown forms. This also raises the question of whether PERG and pupillography can be used in the clinic as meaningful examinations in glaucoma patients.

5. Summary

5.1 Summary

Aim: Many studies have described the functions of ipRGCs, but the interaction between ipRGCs and other retinal cells is not fully understood. However, an interaction between melanopsin, the light sensitive pigment of ipRGCs, and S-cones has been reported (Spitschan et al., 2014). S-cone activity can be recorded as a small positive peak (P) of the transient PERG, recorded with a blue/black checkerboard stimulus after adaptation to a yellow light (Niepel & Dodt, 1989). As S-cones and melanopsin have similar spectral sensitivities, it is possible that melanopsin participates in the S-cone peak of the PERG. Therefore, in this study we sought to correlate this P peak with the activity of melanopsin and to examine whether the PERG to blue stimulation also induces the activity of ipRGCs. For this purpose, we compared recordings of the PERG with those of pupillography parameters, as melanopsin is known to participate in the pupil response. We collected results from healthy volunteers, as well as from patients with glaucoma, who have been shown to have a reduced ipRGC activity (Kankipati et al., 2011).

Methods: Ten healthy volunteers and 10 patients with open-angle glaucoma were examined. Only one eye from each participant was considered. The PERG was performed with a blue / black stimulus, 1 minute and 2 minutes after yellow light adaptation. Pupillography was performed with a blue and a red stimulus after light and dark adaptation. In addition, blood pressure, O^2 and pulse were measured 3 times, i. e. before, between and at the end of the recordings, to ensure that changes in these parameters do not affect the results.

Results: The majority of PERG recordings after yellow light adaptation showed a small peak (P) after the P50 peak with an implicit time between 90-110 msec. The amplitude of P was significantly different between healthy subjects and glaucoma patients in the first minute after light adaptation ($p = 0.018$). The redilation times from the pupillography recordings, significant differences were also found between healthy controls and glaucoma patients after a blue stimulus with light adaptation ($p = 0.047$), as well as after dark adaptation ($p = 0.001$). Moderately positive correlations were

found in healthy volunteers between the amplitude of P and the redilation time with a blue stimulus 2 min after DA (CC = 0.620) and in glaucoma patients 2 min after adaptation with a red or blue stimulus (CC = 0.678 and 0.508, respectively). In the healthy group, there was a moderately negative correlation between P in the first minute after yellow light adaptation and the redilation time with blue stimulus and light adaptation (CC = -0.550).

Discussion: The results corroborate the theory that healthy ipRGCs have an influence on the S-cone peak (P) amplitude in the PERG recordings. The results of the pupillography additionally show that the mean redilation time is higher in the healthy group than in the glaucoma group, except for the blue stimulus with light adaptation. This can be explained by the known influence of ipRGCs on the regulation of pupil function, which is reduced in glaucoma patients. The results suggest a possible indirect participation of ipRGCs in the P-amplitude of the S-cone, but due to several limitations in our study, further studies are necessary to confirm this involvement and to better understand the correlation between ipRGCs and the P amplitude of the S-cone.

5.2 Summary in German

Ziel der Studie: Viele Studien haben Funktionen der ipRGCs beschrieben, aber die Interaktion zwischen ipRGCs und anderen Netzhautzellen ist noch nicht vollständig bekannt.

Es wurde jedoch über eine Interaktion zwischen Melanopsin, dem lichtempfindlichen Pigment von ipRGCs, und S-Cones berichtet (Spitschan et al., 2014). Die S-cone-Aktivität kann als kleiner positiver Peak (P) des transienten PERG mit einem blau/schwarzen checkerboard-Stimulus nach Gelblichtadaptation aufgezeichnet werden,. Da S-cones und Melanopsin ähnliche spektrale Empfindlichkeiten aufweisen, ist es möglich, dass Melanopsin am S-cones-Peak vom PERG teilnimmt. Daher haben wir mit dieser Studie versucht, diesen P-Peak mit der Aktivität von Melanopsin zu korrelieren und zu untersuchen, ob das PERG zu Blaustimulation auch die Aktivität von ipRGCs induziert. Zu diesem Zweck haben wir die Aufzeichnungen vom PERG mit denen der Pupillographie-Parameter verglichen, da bekannt ist, dass Melanopsin an der Pupillenreaktion beteiligt ist. Wir haben Ergebnisse von gesunden Probanden sowie von Patienten mit Glaukom gesammelt, bei denen eine reduzierte ipRGC-Aktivität nachgewiesen wurde (Kankipati et al., 2011).

Methoden: Es wurden 10 gesunde Probanden und 10 Patienten mit Offenwinkelglaukom untersucht. Es wurde nur ein Auge von jedem Teilnehmer berücksichtigt. Das PERG wurde mit einem Blau/Schwarz-Stimulus 1 Minute und 2 Minuten nach Gelblichtadaption durchgeführt. Die Pupillographie wurde mit Blaustimulus und Rotstimulus nach Helladaptation und Dunkeladaptation durchgeführt. Außerdem wurde 3-mal Blutdruck, O2 und Puls gemessen, jeweils vor, zwischen und am Ende der Aufzeichnungen, um sicherzustellen, dass die Änderungen dieser Parameter die Ergebnisse nicht beeinflussen.

Ergebnisse: Die Mehrheit der PERG-Aufzeichnungen nach Gelblichtadaption haben einen kleinen Peak (P) nach dem P50-Peak mit einer impliziten Zeit zwischen 90-110 ms gezeigt. Die Amplitude von P war in der ersten Minute nach der Gelblichtadaption zwischen gesunden Probanden und Glaukompatienten signifikant unterschiedlich ($p = 0.018$). Auch bei den Redilationszeiten aus den Aufzeichnungen der Pupillographie fanden sich signifikante Unterschiede zwischen gesunden Probanden und

Glaukompatienten nach Blaustimulus mit Lichtadaptation (p = 0.047), sowie nach Dunkeladaptation (p = 0.001). Moderate positive Korrelationen wurden bei gesunden Probanden zwischen der Amplitude von P und der Redilationszeit mit einem Blaustimulus 2 min nach DA (CC = 0.620) und bei Glaukompatienten 2 min nach Adaptation mit einem Rotstimulus oder Blaustimulus gefunden (CC = 0,678 und 0,508, respektive). In der gesunden Gruppe zeigte sich eine moderat negative Korrelation zwischen P in der ersten Minute nach Gelblichtadaptation und der Redilatationszeit mit Blaustimulus und Lichtadaptation (CC = -0.550).

Diskussion: Die Ergebnisse bestätigen die Theorie, dass gesunde ipRGCs einen Einfluss auf die S-Cone-Peak (P)-Amplitude in den PERG-Aufzeichnungen haben. Die Ergebnisse der Pupillographie zeigen zudem, dass der Mittelwert der Redilatationszeit bei der gesunden Gruppe höher ist als bei der Glaukomgruppe, mit Ausnahme des Blaustimulus mit Lichtadaptation. Dies kann durch den bekannten Einfluss von ipRGCs auf die Regulation der Pupillenfunktion geklärt werden, der bei Glaukompatienten reduziert ist. Die Ergebnisse deuten auf eine mögliche indirekte Beteiligung von ipRGCs an der P-Amplitude vom S-Cone hin. Aufgrund mehrerer Einschränkungen in unserer Studie sind jedoch weitere Studien notwendig, um diese Beteiligung zu bestätigen und die Korrelation zwischen ipRGCs und der P-Amplitude der S-Cone besser zu verstehen.

6. Appendix

6.1 Figures

6.2 Tables

6.3 Individual PERGs' results from glaucoma patients

n	1	2	3	4	5	6	7	8	9	10
Gender	m	f	m	f	m	f	m	f	m	m
eye	OD	OS	OS	OS	OS	OD	OD	OD	OS	OS
Amp P50 no	2.31	1.28	1.59	1.47	2.78	1.7	2.53	1.68	1.41	0.83
Amp P50 yes1	2.25	1.36	1.12	1.09	0.46	0.91	1.59	1.15	2.04	0.39
Amp P50 yes2	4.39	1.51	0.73	1.25	2.45	1.05	0.67	1.78	2.07	0.39
Imp P50 no	67	45.5	52.5	48.5	54	57.5	55.5	67	58	58
Imp P50 yes1	68	53.	46	55	61	55	64.5	65	57	51.5
Imp P50 yes2	76	61.5	52.	52.5	55	53	62.5	54	56	39.5
P Amp yes1	2.17	0.88	0.73	0.8	0.29	0.58	1.23	-0.42	1.02	0.19
P Amp yes2	2.64	1.04	0.34	0.59	1.06	0.24	-0.02	1.35	0.65	0.18
P Imp yes1	86	77	57.5	77	62.5	68.5	79	78	74	64
P Imp yes2	92	78	68	64	74.5	66.5	87	72.5	65	60.5
N95 Amp no	2.19	-1.13	-1.79	-1.79	-4.37	-2.07	-2.4	-2.33	-1.24	-1.26
N95 Amp yes1	0.71	-2.12	-1.1	-2.28	-1.28	-1	-2.76	-1.12	-2.49	-0.58
N95 Amp yes2	-2.3	-1.53	-1.3	-2.11	-3.97	-1.88	-1.39	-1.09	-2.75	-0.72

Abbreviations: PERG: pattern electroretinogram, N: number of subject, m: male, f: female, Amp: amplitude, Imp: implicit time, no: without yellow adaptation, yes1: is the PERG measure 1 minute after yellow light adaptation, yes2: is the PERG measure after 2 minutes of yellow adaptation.

7. References

Adhikari, P., Feigl, B. & Zele, A. J. (2016) Rhodopsin and Melanopsin Contributions to the Early Redilation Phase of the Post-Illumination Pupil Response (PIPR. PLoS One, 11(8), e0161175. https://doi.10.1371/journal.pone.0161175

Bach, M., Brigell, M. G., Hawlina, M., Holder, G. E., Johnson, M. A., McCulloch, D. L., Meigen, T., & Viswanathan, S. (2013). ISCEV standard for clinical pattern electroretinography (PERG): 2012 update. Doc. Ophthalmal., 126 (1), 1–7.

https://doi.org/10.1007/s10633-012-9353-y

Bach, M., Cuno, A. K., & Hoffmann, M. B. (2018). Retinal conduction speed analysis reveals different origins of the P50 and N95 components of the (multifocal) pattern electroretinogram. Exp. Eye Res., 169, 48–53.

https://doi.org/10.1016/j.exer.2018.01.021

Bellini, G., Bocin, E., Cosenzi, A., Sacerdote, A., Molino, R., Solimano, N., & Ravalico, G. (1995). Oscillatory potentials of the electroretinogram in hypertensive patients. Hypertension (Dallas, Tex. : 1979), 25(4 Pt 2), 839–841.

https://doi.org/10.1161/01.hyp.25.4.839

Berson, D. M., Dunn, F. A., & Takao, M. (2002). Phototransduction by retinal ganglion cells that set the circadian clock. Science, 295(5557), 1070–1073.

https://doi.org/10.1126/science.1067262

Chan, R. Y., & Naka, K. (1976). The amacrine cell. Vision Res., 16(10), 1119–1129. https://doi.org/10.1016/0042-6989(76)90252-2

Cui, Q., Ren, C., Sollars, P. J., Pickard, G. E., & So, K. F. (2015). The injury resistant ability of melanopsin-expressing intrinsically photosensitive retinal ganglion cells. Neuroscience, 284, 845–853. https://doi.org/10.1016/j.neuroscience.2014.11.002

Cvenkel, B., Sustar, M., & Perovšek, D. (2017). Ganglion cell loss in early glaucoma, as assessed by photopic negative response, pattern electroretinogram, and spectral-domain optical coherence tomography. Doc. Ophthalmal., 135(1), 17–28. https://doi.org/10.1007/s10633-017-9595-9

Dacey, D. M., Liao, H. W., Peterson, B. B., Robinson, F. R., Smith, V. C., Pokorny, J., Yau, K. W., & Gamlin, P. D. (2005). Melanopsin-expressing ganglion cells in primate retina signal colour and irradiance and project to the LGN. Nature, 433 (7027), 749–754. https://doi.org/10.1038/nature03387

Dowling, J. E., & Boycott, B. B. (1966). Organization of the primate retina: electron microscopy. Proc. Roy. Soc. Lond. Ser.-B, Bio., 166(1002), 80–111.

https://doi.org/10.1098/rspb.1966.0086

Duke-Elder, S & Wybar, KC. (1961). System of Ophthalmology: Volume II, the

Anatomy of the Visual System. CV Mosby.

Ecker, J. L., Dumitrescu, O. N., Wong, K. Y., Alam, N. M., Chen, S. K., LeGates, T.,

Renna, J. M., Prusky, G. T., Berson, D. M., & Hattar, S. (2010). Melanopsin-expressing retinal ganglion-cell photoreceptors: cellular diversity and role in pattern vision. Neuron, 67(1), 49–60.

https://doi.org/10.1016/j.neuron.2010.05.023

Estevez, M. E., Fogerson, P. M., Ilardi, M. C., Borghuis, B. G., Chan, E., Weng, S.,

Auferkorte, O. N., Demb, J. B., & Berson, D. M. (2012). Form and function of the M4 cell, an intrinsically photosensitive retinal ganglion cell type contributing to geniculocortical vision. The Journal of neuroscience : the official journal of the Society for Neuroscience, 32(39), 13608–13620.

https://doi.org/10.1523/JNEUROSCI.1422-12.2012

Freedman, M. S., Lucas, R. J., Soni, B., von Schantz, M., Muñoz, M., David-Gray, Z., & Foster, R. (1999). Regulation of mammalian circadian behavior by non-rod, non-cone, ocular photoreceptors. Science, 284(5413), 502–504.

https://doi.org/10.1126/science.284.5413.502

Gamlin, P. D., McDougal, D. H., Pokorny, J., Smith, V. C.,Yau, K. W., Dacey, D. M. (2007) Human and macaque pupil responses driven by melanopsin-containing retinal ganglion cells. Vision Res., 47(7), 946-54.

https://doi.org/10.1016/j.visres.2006.12.015

Gooley, J. J., Lu, J., Chou, T. C., Scammell, T. E., & Saper, C. B. (2001). Melanopsin in cells of origin of the retinohypothalamic tract. Nature Neurosci., 4(12), 1165. https://doi.org/10.1038/nn768

Gordon, P. S., Kostic, M., Monsalve, P. F., Triolo, G., Golubev, L., Luna, G., Ventura, L. M., Feuer, W. J., & Porciatti, V. (2020). Long-term PERG monitoring of untreated and treated glaucoma suspects. Doc. Ophthalmol.,141(2), 149–156.

https://doi.org/10.1007/s10633-020-09760-5

Hannibal, J., Hindersson, P., Ostergaard, J., Georg, B., Heegaard, S., Larsen, P. J., & Fahrenkrug, J. (2004). Melanopsin is expressed in PACAP-containing retinal ganglion cells of the human retinohypothalamic tract. Invest. Ophthalmol. Vis. Sci., 45(11), 4202–4209. https://doi.org/10.1167/iovs.04-0313

Hatori, M., Le, H., Vollmers, C., Keding, S. R., Tanaka, N., Buch, T., Waisman, A., Schmedt, C., Jegla, T., & Panda, S. (2008). Inducible ablation of melanopsin-expressing retinal ganglion cells reveals their central role in non-image forming visual responses. PloS One, 3(6), e2451.

https://doi.org/10.1371/journal.pone.0002451

Hattar, S., Liao, H. W., Takao, M., Berson, D. M., & Yau, K. W. (2002). Melanopsin-containing retinal ganglion cells: architecture, projections, and intrinsic photosensitivity. Science, 295(5557), 1065–1070.

https://doi.org/10.1126/science.1069609

Henkes, H. E., Van Der Kam, J. P. & Westhoff, A. J. S. (1954).). Electroretinographic studies in arterial hypertension: Effect of reduction in blood pressure on electrical response of human retina.

https://jamanetwork.com/journals/jamaophthalmology/article-abstract/624116

Hopkins, J. M., & Boycott, B. B. (1997). The cone synapses of cone bipolar cells of primate retina. J. Neurocytol., 26(5), 313–325.

https://doi.org/10.1023/a:1018504718282

Jeon, S. J., Park, H. L., Jung, K. I., & Park, C. K. (2019). Relationship between pattern electroretinogram and optic disc morphology in glaucoma. PloS One, 14(11), e0220992. https://doi.org/10.1371/journal.pone.0220992

Jung, K. I., Jeon, S., Shin, D. Y., Lee, J., & Park, C. K. (2020). Pattern Electroretinograms in Preperimetric and Perimetric Glaucoma. Am. J. Ophthalmol., 215, 118–126. https://doi.org/10.1016/j.ajo.2020.02.008

Kankipati, L., Girkin, C. A., & Gamlin, P. D. (2011). The post-illumination pupil response is reduced in glaucoma patients. Invest. Ophthalmol. Vis. Sci., 52(5), 2287–2292. https://doi.org/10.1167/iovs.10-6023

Kawasaki, A., & Kardon, R. H. (2007). Intrinsically photosensitive retinal ganglion cells. J. Neuro-Ophthalmol., 27(3), 195–204. https://doi.org/10.1097/WNO.0b013e31814b1df9

Kergoat, H., & Forcier, P. (1996). Correlation of an exercise-induced increase in systemic circulation with neural retinal function in humans. Documenta ophthalmologica. Advances in ophthalmology, 92(3), 145–157. https://doi.org/10.1007/BF02583286

Kolb, H., Nelson, R., & Mariani, A. (1981). Amacrine cells, bipolar cells and ganglion cells of the cat retina: a Golgi study. Vision Res., 21(7), 1081–1114. https://doi.org/10.1016/0042-6989(81)90013-4

KUFFLER S. W. (1953). Discharge patterns and functional organization of mammalian retina. Journal of neurophysiology, 16(1), 37–68. https://doi.org/10.1152/jn.1953.16.1.37

Lee, S. K., & Schmidt, T. M. (2018). Morphological Identification of Melanopsin-Expressing Retinal Ganglion Cell Subtypes in Mice. Methods in molecular biology (Clifton, N.J.), 1753, 275–287. https://doi.org/10.1007/978-1-4939-7720-8_19

Lee, S. K., Sonoda, T., & Schmidt, T. M. (2019). M1 Intrinsically Photosensitive Retinal Ganglion Cells Integrate Rod and Melanopsin Inputs to Signal in Low Light. Cell reports, 29(11), 3349–3355.e2. https://doi.org/10.1016/j.celrep.2019.11.024

MacNichol, E. J., & Svaetichin, G. (1958). Electric responses from the isolated retinas of fishes. Am. J. Ophthalmol., 46(3 Part 2), 26–46. https://doi.org/10.1016/0002-9394(58)90053-9

Masland R. H. (2001). The fundamental plan of the retina. Nature Neurosci., 4(9), 877–886. https://doi.org/10.1038/nn0901-877

McDougal, D. H., & Gamlin, P. D. (2010). The influence of intrinsically-photosensitive retinal ganglion cells on the spectral sensitivity and response dynamics of the human pupillary light reflex. Vision research, 50(1), 72–87.

https://doi.org/10.1016/j.visres.2009.10.012

Nakatsuka, K., & Hamasaki, D. I. (1985). Destruction of the indoleamine-accumulating amacrine cells alters the ERG of rabbits. Investigative ophthalmology & visual science, 26(8), 1109–1116.

Nicholls, J. G., Martin, R. A. & Wallace, B. G. (1992). From Neuron to Brain: A Cellular and Molecular Approach to the Function of the Nervous System: Cellular Approach to the Function of the Nervous System (3rd Aufl.). Sinauer Associates Inc.,U.S.

Park, J. C., Moura, A. L., Raza, A. S., Rhee, D. W., Kardon, R. H., & Hood, D. C. (2011). Toward a clinical protocol for assessing rod, cone, and melanopsin contributions to the human pupil response. Investigative ophthalmology & visual science, 52(9), 6624–6635. https://doi.org/10.1167/iovs.11-7586

Porciatti. V. (2015). Electrophysiological assessment of retinal ganglion cell function. Exp. Eye Res., 141, 164–170. https://doi.org/10.1016/j.exer.2015.05.008

Provencio, I., Jiang, G., De Grip, W. J., Hayes, W. P., & Rollag, M. D. (1998). Melanopsin: An opsin in melanophores, brain, and eye. P. Natl. Acad. Sci. USA, 95(1), 340–345. https://doi.org/10.1073/pnas.95.1.340

Provencio, I., Rodriguez, I. R., Jiang, G., Hayes, W. P., Moreira, E. F., & Rollag, M. D. (2000). A novel human opsin in the inner retina. The Journal of neuroscience : the official journal of the Society for Neuroscience, 20(2), 600–605.

https://doi.org/10.1523/JNEUROSCI.20-02-00600.2000

Rukmini, A. V., Milea, D., & Gooley, J. J. (2019). Chromatic Pupillometry Methods for Assessing Photoreceptor Health in Retinal and Optic Nerve Diseases. Front. Neurol., 10, 76. https://doi.org/10.3389/fneur.2019.00076

Schmidt, T. M., Do, M. T., Dacey, D., Lucas, R., Hattar, S., & Matynia, A. (2011). Melanopsin-positive intrinsically photosensitive retinal ganglion cells: from form to function. J. Neurosci., 31(45), 16094–16101.

https://doi.org/10.1523/JNEUROSCI.4132-11.2011

Senger, C., Moreto, R., Watanabe, S., Matos, A. G., & Paula, J. S. (2020). Electrophysiology in Glaucoma. J. Glaucoma, 29(2), 147–153.

https://doi.org/10.1097/IJG.0000000000001422

Shand J., Foster R.G. (1999). The extraretinal photoreceptors of non-mammalian vertebrates. In: Archer S.N., Djamgoz M.B.A., Loew E.R., Partridge J.C., Vallerga S. (eds) Adaptive Mechanisms in the Ecology of Vision. Springer, Dordrecht. https://doi.org/10.1007/978-94-017-0619-3_7

Spitschan, M., Jain, S., Brainard, D. H., & Aguirre, G. K. (2014). Opponent melanopsin and S-cone signals in the human pupillary light response. P. Natl. Acad. Sci. USA, 111(43), 15568–15572. https://doi.org/10.1073/pnas.1400942111

Tatham, A. J., Meira-Freitas, D., Weinreb, R. N., Zangwill, L. M., & Medeiros, F. A. (2014). Detecting glaucoma using automated pupillography. Ophthalmol. 121(6), 1185–1193. https://doi.org/10.1016/j.ophtha.2013.12.015

Torse, D.A., Maggavi, R., & Pujari, S. (2012). Nonlinear Blind Source Separation for EEG Signal Pre-processing in Brain-Computer Interface System for Epilepsy. International Journal of Computer Applications, 50, 12-19.

Warren, E.J., Allen, C.N., Brown, R.L. and Robinson, D.W. (2003), Intrinsic light responses of retinal ganglion cells projecting to the circadian system. Eur. J. Neurosci., 17: 1727-1735. https://doi.org/10.1046/j.1460-9568.2003.02594.x

Watanabe, M., & Rodieck, R. W. (1989). Parasol and midget ganglion cells of the primate retina. J. Comp. Neurol., 289(3), 434–454.

https://doi.org/10.1002/cne.902890308

West, E. L., Pearson, R. A., Tschernutter, M., Sowden, J. C., MacLaren, R. E., & Ali, R. R. (2008). Pharmacological disruption of the outer limiting membrane leads to increased retinal integration of transplanted photoreceptor precursors. Experimental eye research, 86(4), 601–611. https://doi.org/10.1016/j.exer.2008.01.004

Wilhelm, H., & Wilhelm, B. (2003). Clinical applications of pupillography. J. Neuro-Ophthalmol., 23(1), 42–49. https://doi.org/10.1097/00041327-200303000-00010

Willoughby, C., Ponzin, D., Ferrari, S., Lobo, A., Landau, K., & Omidi, Y. (2010). Anatomy and physiology of the human eye: effects of mucopolysaccharidoses disease on structure and function - a review. Clinical and Experimental Ophthalmology, 38(SUPPL. 1), 2-11.

https://doi.org/10.1111/j.1442-9071.2010.02363.x

Yoshimura, N. & Hangai, M. (2014). OCT Atlas. Springer Publishing.

Young, R. S., & Kennish, J. (1993). Transient and sustained components of the pupil response evoked by achromatic spatial patterns. Vision Res., 33(16), 2239–2252. https://doi.org/10.1016/0042-6989(93)90103-4

Zrenner, E., Nelson, R., & Mariani, A. (1983). Intracellular recordings from a biplexiform ganglion cell in macaque retina, stained with horseradish peroxidase. Brain Res., 262(2), 181–185. https://doi.org/10.1016/0006-8993(83)91007-7

8. Declaration

I, Mohammad Aloudat, confirm that the work presented in this thesis is my own. Where information has been derived from other sources, I confirm that this has been indicated in the thesis.

Mohammad Aloudat
September 2023